Emerging Trends in Engineering and Technology

Volume - 6

Chief Editor

Mohit Bajpai
Associate Professor, Electronics and Communication Engineering, Poornima Institute of Engineering & Technology, Jaipur, Rajasthan, India

Co-Editor

Dr. A.V. Sudhakara Reddy
Associate Professor, R&D Coordinator, Department of Electrical and Electronics Engineering, Malla Reddy Engineering College (Autonomous), Maisammaguda, Secunderabad, Telangana, India

Dr. V. Lakshmi Devi
Professor, Department of EEE, S.V. College of Engineering, Tirupati, Andhra Pradesh, India

Integrated Publications ™
New Delhi

Published By: Integrated Publications

Integrated Publications
H. No. - 3 Pocket - H34, Sector - 3,
Rohini, Delhi-110085, India

Chief Editor: Mohit Bajpai
Co-Editor: Dr. A.V. Sudhakara Reddy and Dr. V. Lakshmi Devi

Publication Year: 2022

Pages: 111

ISBN: 978-93-93502-45-2

Book DOI: https://doi.org/10.22271/int.book.208

Price: ₹ 706/-

Contents

Chapter - 1

MANETs, Routing Protocols and Mobility Models

Authors

Dr. Satveer Kour

Assistant Professor, Department of Computer Engineering and Technology, Guru Nanak Dev University, Amritsar, Punjab, India

Er. Sandeep Kaur

Assistant Professor, Department of Computer Engineering and Technology, Guru Nanak Dev University, Amritsar, Punjab, India

Dr. Satinder Kaur

Assistant Professor, Department of Computer Engineering and Technology, Guru Nanak Dev University, Amritsar, Punjab, India

Chapter - 1

MANETS, Routing Protocols and Mobility Models

Dr. Satveer Kour, Er. Sandeep Kaur and Dr. Satinder Kaur

Abstract

Since 1970's, Wireless Networks systems are continuously providing pervasive computing capability and information access to mobile users without concerning location. It came in two variations: infrastructure and no-infrastructure. The internet is wireless ad-hoc network (no-infrastructure) stems from of their well-known advantages for certain types of applications. Since, there is no fixed infrastructure; a wireless ad-hoc network can be deployed quickly. Thus, such networks can be used in situations where either there is no other wireless communication infrastructure present or where such infrastructure cannot be used because of security, cost, or safety reasons. Such a network is tolerant of failure or departure of terminals, because the network does not rely on a few critical terminals for its organization or control. Similarly, terminals can be added easily to the network. The main applications lie in immediate communication in 'harse' environments, where there is no time or resource for laying down the wired infrastructure. Applications such as rescue missions in times of natural disasters, law enforcement operation, commercial and educational use, and sensor networks are just few possible commercial examples.

Keywords: Wireless networks, MANETs, routing protocols, mobility models

1.1 Introduction

The wireless infrastructure networks, or cellular network [1], hold a centralized entity. The fixed connected base stations are used to exchange information to other fixed base stations via guided media. The communication range of a base station makes a cell as shown in figure 1.1. The mobile nodes of a cell communicate to the closest base station. The situation of a mobile node goes beyond the range of a base station is called handoff. In this situation, the moving node connects to the next central station [2]. The no-infrastructure network or Mobile Ad-hoc Network

(MANET) has not any centralized entity as presented in figure 1.2. The nodes can go forward and communicate with other nodes. A terminal is fully responsible for organizing and controlling the system. The complete system is mobile, and each terminal can move of its own choice [3]. A multi-hop property is used for long range of users. The device in this network will perform as a router for a route establishment. A node may lie at airplanes, trucks, ships or any other moving devices [4].

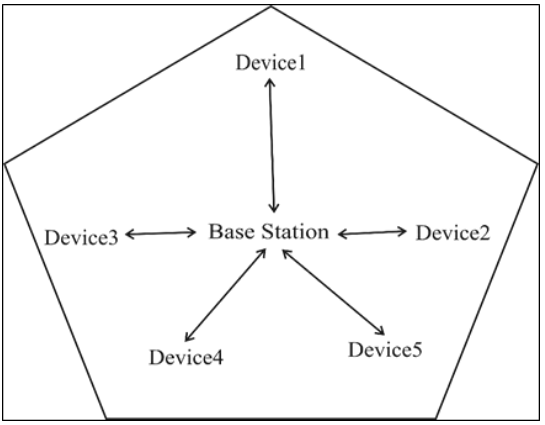

Fig 1.1: Cellular Network [3]

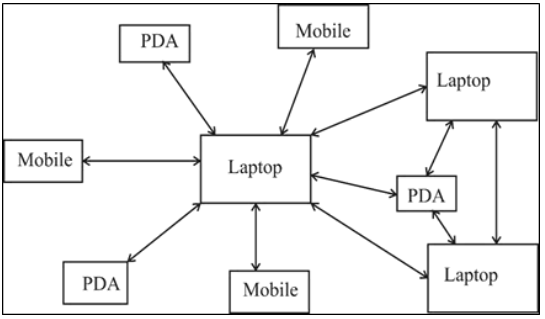

Fig 1.2: No-Infrastructure Network [4]

1.1.1 Advantages of wireless network

The wireless network has many advantages for small businesses, including:

- **Convenience:** From any location, network resources accessibility is possible.
- **Mobility:** Unlike wired connection, you can move from your location.

- **Productivity:** Internet facility helps to an organization's critical applications and resources of staff to complete the job.
- **Easy Setup:** There is no need of string cables and installation performs quickly with effective cost.
- **Expandable:** The wireless networks can be easily expanded, whereas additional wiring is required in a wired network.
- **Security:** Security protections are more robust in wireless networks [5].
- **Cost:** A wireless network cost less as compared to wired networks.

1.2 Overview of mobile Ad-Hoc networks

Based on these features, standard cellular networks and wireless fully connected networks do not qualify as ad-hoc networks [6]. Probably, the chief difference between ad hoc networks is the apartment lacks of a centralized entity within an ad-hoc network. These are no base stations or mobile switching centers in an ad-hoc network.

The internet is wireless ad-hoc network stems from of their well-known advantages for certain types of applications [7]. Since, there is no fixed infrastructure; a wireless ad-hoc network can be deployed quickly. Thus, such networks can be used in situations where either there is no other wireless communication infrastructure present or where such infrastructure cannot be used because of security, cost, or safety reasons. Such a network is tolerant of failure or departure of terminals, because the network does not rely on a few critical terminals for its organization or control. Similarly, terminals can be added easily to the network [8]. The main applications lie in immediate communication in 'harse' environments, where there is no time or resource for laying down the wired infrastructure. Applications such as rescue missions in times of natural disasters, law enforcement operation, commercial and educational use, and sensor networks are just few possible commercial examples [9, 10].

A web of wireless devices free from any centralized entity is considered as a Mobile Ad-Hoc Network (MANET) [11]. A device may connect directly with other devices through wireless links. The concept of multi-hop routing is used for those nodes which are far from other nodes [12]. The intermediate nodes are called relay nodes. It is different from a wired network due to lack of a centralized entity. The fixed base stations do not exist in the structure. An illustration of such kind of network is an Internet. A leading research has covered the study of protocols and algorithms [13]; it becomes harder to

decide, which algorithm is preferable to others under and what conditions [14].

1.3 Characteristics of MANETs

- **Dynamic topologies:** The physical arrangement of nodes may vary frequently and rapidly at random times [15].
- **Ad-hoc topology: N**o fixed physical arrangement of the scenario is there [16].
- **Links with lower capacity:** The connections have low power capacity than connected links. The throughput will be low due to interference conditions, multiple accesses, and fading noise etc.
- **Energy constrained operation:** More physical security threats are there for some or all of the nodes than the fixed networks. It increases spoofing, attacks, and eavesdropping for these networks.
- **Mobility:** A node in the network can travel independently or in a group through some mobility model [16, 17, 18].
- **Wireless network:** By nature, MANETs are also wireless networks. Most of the research currently being conducted in MANET routing protocols use the 802.11 MAC address [19].

MANETs are of two types [20] namely homogeneous MANET as shown in figure 1.11 and the heterogeneous MANET as shown in figure 1.12. Such systems are well suited for infrastructure less applications such as space exploration, military communication systems, marine operations, rescue operations, and environmental monitoring. The use of MANET is comparatively cheaper than wired networks.

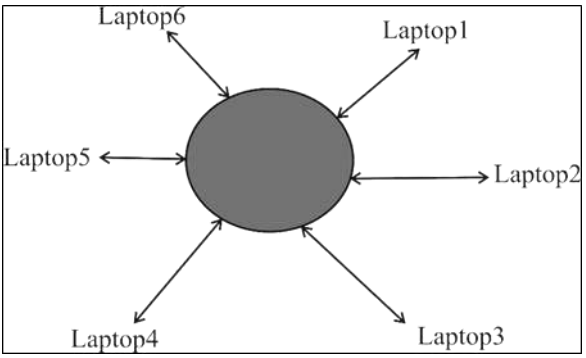

Fig 1.11: Homogeneous MANET

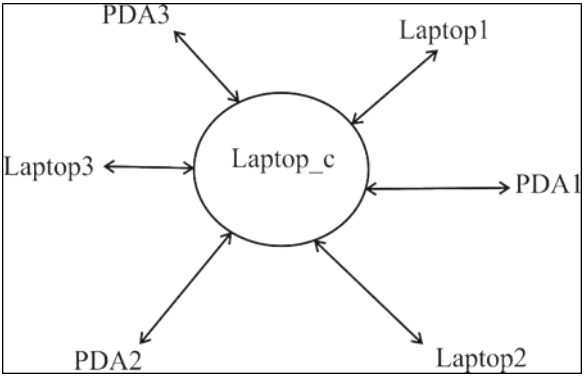

Fig 1.12: Heterogeneous MANET

The U.S. Defense Research Agency supported the project named as Packet Radio Network (PRNET) [21] that was the starting of ad-hoc networks. Next, a Survivable Radio Network (SURAN) project was launched in the year 1980. It established and maintained an automatic call in PRNET with low mobility. It grew in the nineties due to portable equipment. It also merged the concept of internetworking protocols for MANETs. Then, Internet Engineering Task Force was introduced for those protocols [22] which were IP based. The Department of Defense (DoD) also renewed their support for Global Mobile Information Systems Network Simulator (GloMoSim) and radio projects like Near-term Digital Radio (NTDR). In 1995, MAC protocol and 802.11 physical layers were developed. Nowadays, any user can make an ad hoc Network by just inserting in 802.11 Personal Computer Memory Card International Association (PCMCIA) cards with laptops.

Milestones in the history of data networking include the airline reservation system application in the 1960s, Ethernet was developed in the 1970s, LANs were introduced on stand-alone micro computers in 1980s, and improved mobile or wireless devices and networks connected to an organizational Network in 2000s. Up to 2007, 500 million computers were connected to the Internet. Smart phones and tablets show a very strong growth rate in year 2010. Another trend that is rapidly affecting is the growth of smaller devices to connect to the Internet. Tablets, thermostats, and even light bulbs are now capable of tapping into the web on the go [23]. The Internet of Things (IoT) is adding devices, too. As the Internet has become ubiquitous, faster, and increasingly accessible to non-technical communities, social networking and collaborative services have grown rapidly, enabling people to communicate and share interests in many more ways. Sites like

Facebook, Twitter, Linked-In, YouTube, Flickr, Second Life, blogs, Instagram, wikis, and many more let people of all ages rapidly share their interests of the moment with others everywhere. It has provided a huge boost to the genealogy industry. Protecting privacy is quite a challenge in this environment.

1.4 MANETs: Advantages and Applications

Advantages

- Simple, fast and cheap setup of networks.
- Transmit power can be reduced compared to wireless infrastructure networks.
- More robust concerning a failure of single components due to decentralized structure.

Military applications

- Formations of soldiers, tanks, planes.

Civil applications

- Conferences, exhibitions, meetings, lecturers.
- Telematics applications in traffic.
- Extension of cell-based systems like WLANs, Universal Mobile Telecommunications Service (UMTS).
- Entertainment on travels (file sharing, gaming in trains, cars, or planes).
- Sports events.
- Networks for cabs, and police.
- Sensor networks.

1.5 Routing protocols

To discover a path between mobile nodes, the process of routing is performed. In ad-hoc networks, nodes are not familiar with the topology of their networks. They have to discover the route by announcing its presence and listens for announcements broadcast by its neighbors. There is the concept of a mobile agent, home agent, home network, foreign agent, and the foreign network. In case of handoff by the mobile agent, it informs the home network. Its home agent then forwards its messages to the agents of the foreign network. A mobile agent registers itself to the external network with the foreign agent. So, all the data forwarded to the assistant existed on the

external network to the registered node. The previous settings are restored on the returning of a mobile agent to its local network. The foreign network nodes are not involved for the details regarding the movement of a mobile agent. But in MANETs, the home agent is moving. The node-by-node routing relies on existing routing protocols as in a wired network and is shown in figure 1.13 [24].

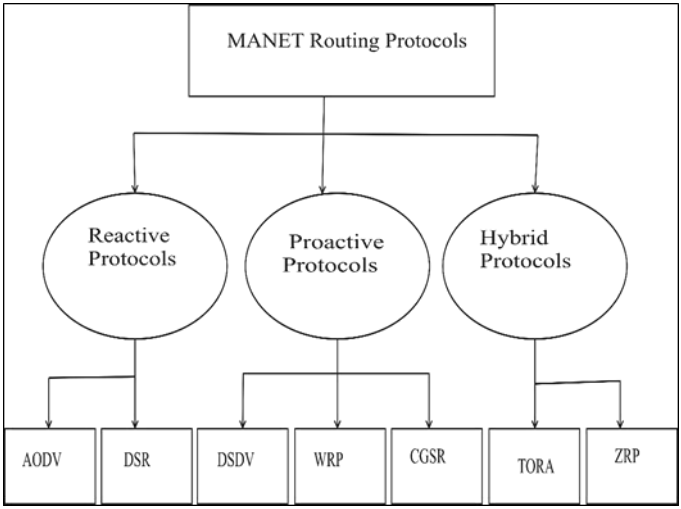

Fig 1.13: Categorization of Protocols for Routing [25]

1.5.1 Protocols for reactive routing

Such protocols are important for the temporarily organized network. The cause is neither sending advertisements nor receiving advertisements so that the battery backup is saved. A table of routing is created by each node to save the routes. The table kept only valid entries and the old entries are removed after an active route timeout. A serious problem with MANETs occurs when connection failures occur due to mobility of the devices. The path establishment operation significantly increases the broadcast traffic in the environment. Figure 1.14 depicts the route configuration process by a reactive routing protocol.

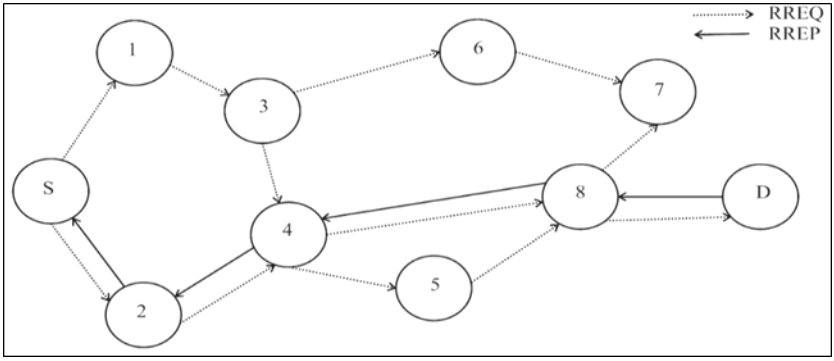

Fig 1.14: Route Discovery Process

1.5.1.1 Ad-Hoc On Demand Distance Vector (AODV)

It establishes a path on request only [26] due to its reactive property. It does not maintain the route of destinations not used by nodes. It confirms loop-free paths by using sequence number to show an indication about the freshness of a route. Every node saves a table to identify a single path entry for the target node with whom the node is communicating. Each entry consists of following:

- IP address of a target
- Sequence number of target
- Neighbour
- Total neighbours
- Address lifetime
- Status flags

Path finding

The originator node announces a packet named as Route Request (RREQ) to its next hops to find the route. As soon as, the neighbor gets this message; it modifies the routing table and also creates route entry for a reverse. A neighbor may unicast a Route Reply (RREP) message in two cases: by the target node or may be the intermediate device to the destination. If any case is true, the next node sends an RREP packet to the originator in a reverse manner. The intermediate hops make routes to the target node. Each device saves the address of the origin along with a sequence number of RREQs with the time PATH_DISCOVERY_TIME keeps a cache where it saves the last received RREQs packet with origin's address and sequence number of received RREQs. A RREQ packet with the

same detail will be discarded. A ring technique is used when a route is searched to the destination node to avoid necessary RREQs. This action performs by a Time to Live (TTL) value. A start TTL values is associated with the first RREQ packet. A TTL value defines the maximum neighbors between the paths from origin to target. The maximum time to receive the RREP is already set. If time outs, then the source node again resends the RREQ packet. This process continues up to the receiving of first RREP or until TTL reaches to NET_DIAMETER value which is called as a route search of a network-wide. The source node tries for a maximum of retries.

Path maintenance

The complete route designates as an invalid route for a link breakage case. A routing error (RERR) message is broadcasted by the node to its neighbors with TTL value initialized to one. This message includes the address of every reachable target. When a node gets an RERR packet, it will search in its cached table. If any route found to invalid, the node sends RERR message to its next hops. When either the destination or some intermediate node moves, a RERR message is sent to the affected source nodes. This RERR is started by the node upstream of the break. The whole process repeats until the source receives a RERR message.

1.5.1.2 Dynamic Source Routing (DSR)

It uses the base of origin routing to send packets. A complete hop sequence must be known before starting the transmission. The path finding process is same as of AODV means requests route only when needs [27]. Every node has a route cache memory to save the routes. If the path is already saved in the routing table, transmission starts; otherwise route discovery process starts. The neighbor reads RREQ only in case of address not in the routing table. An origin computes the complete path up to the destination for travelling. The drawback of source routing is the increased overhead. Since finding a way is an expensive task in terms of energy, time, and bandwidth, the whole route is investigated by a single vertex only, so the resultant route is loop free.

Path discovery

When an origin requests for a link to the target node, then the path finding process is initiated. An origin tracks in its cache for already existing paths. If it is found, this path is used for transmission. If not, the node starts the path making process by sending RREQ messages. The RREQ message with a unique ID also contains the source and destination addresses.

An intermediate receives a path request message; it will look up in its cache memory for a path. It concatenates its entry to the map record of the RREQ message in case of path failure. Then, it conveys this RREQ packet to its next hops. This packet propagates throughout the environment to reach to the target node or to an intermediate node. Then an RREP message is sent along with back route information to the originator.

Path maintenance

Route maintenance handles the situation of link breakage. When any node finds a transmission problem, it deletes the path from its routing problem and creates a path error packet. This RERR message is broadcasted to every node which is involved in data transmission. When the neighboring nodes receive a RERR message, it deletes hop by mistake from its routing table. An acknowledgment message is used to check the status of route links. If an automatic acknowledgment is not feasible, then DSR software acknowledgment is used.

1.5.1.3 Dynamic MANET On Demand (DYMO)

It facilitates multiple hops routing with unicast facility. It makes routing between those DYMO routers whose are participating in the transmission. The source's DYMO router starts circulation of a RREQ messages throughout the scenario to find a path. As soon as, the DYMO router gets the request packet, it replies response packet to the origin. A bi-directional route can be created between originator's DYMO router and the destination DYMO router on the receiving of RREP message by the originator's DYMO router [28]. When a topology changes, the nodes maintain their paths and keep monitoring their links. An error message will send to the originator in the case of a data packet sent over a no longer available link. A path discovery process initiates again on the receiving of RERR message by the source node [29].

1.5.2 Protocols for proactive routing

This scheme is determined as table-driven approach. A device periodically records the details of all the nodes existing in the network. So, when an originator needs to carry transmission of packets; a root is already available. Due to this property, there is no delay in the searching procedure. In the case of high mobility scenario, a proactive scheme spends a lot of time to keep routing information accurate [30]. The network performance becomes small when the link breakage rate is maximized because of a high rate of updating in the cached table.

1.5.2.1 Distance Vector Destination Sequenced (DSDV)

The well-known distributed Bellman-Ford algorithm is the base of DSDV. Each node records its routing table with a next node entry and the total node count for all reachable targets. It works on bi-directional links and does not support unidirectional. To prevent looping, it supports the concept of sequence numbers. The destination node originates the sequence number. DSDV periodically broadcasts route advertisement of the advertising node to keep routing information correct and consistent. A message carries the destination address, next node information, and a total node count to that target. When a neighboring node gets an announcement, it modifies its routing cache. The greater value of the sequence number is a latest route. In the case of sequence number equality, a route with low count value is kept. The receiver increases the hop count value by one. Then the receiving node passes this information within its route advertisement [31].

On the link failure, the node marks all routes linked with the route with a hop count of infinity and scatters modified information. It is considered to be correct with the greater sequence number. This is the reason of assigning odd sequence numbers for detecting failure. This process increases overhead, introduces DSDV two kinds of path updating packets. A full dump message containing the complete information and smaller increment packet contains information to broadcast information since a last dump [32].

1.5.2.2 Optimized Link State Routing (OLSR)

It uses the following steps to find the path;

1) It periodically sends a message named as HELLO for getting information from its neighbors.
2) It floods control packets using relays for multiple points.
3) Execute shortest path algorithm for selecting the path.

Each node with its two step neighbor's is accessible. MPR nodes send messages which are rebroadcasted by the nodes. It automatically controls the packet overhead. Every node uses a partial topology graph. A relay node forwards control topology packets to show its existence to its relay selectors. The shortest path first algorithm is frequently used by the origin for finding optimized route [33, 34].

1.5.3 Hybrid Routing Protocols (HRP)

These protocols concatenate on the table and demand routing on a single platform. An HRP is used to find out the optimized routes up to destinations.

This is also called balanced hybrid routing. The routing is initially established with some proactively prospected routes and then serves the demand from additionally activated nodes through reactive flooding.

1.5.3.1 Zone Routing Protocol (ZRP)

It treats as a table driven while finding of routes within a local zone. It uses on-demand property for making communication in between these zones. The Intra-zone Routing Protocol (IARP), or a proactive routing protocol, is used inside routing zones. The Inter-zone Routing Protocol (IERP), or a reactive routing protocol, is used between routing zones. These pure properties have their distinct drawbacks. It must follow different approaches to separate the nodes from a local neighborhood from the global neighborhood. These local areas pronounce as zones. A node may move between multiple zones. Each zone has its different size which is described by a radius, *r*. A radius *r* is the counting of neighbors reachable from the origin node [35]. The radius with r=2 is shown in figure 1.15.

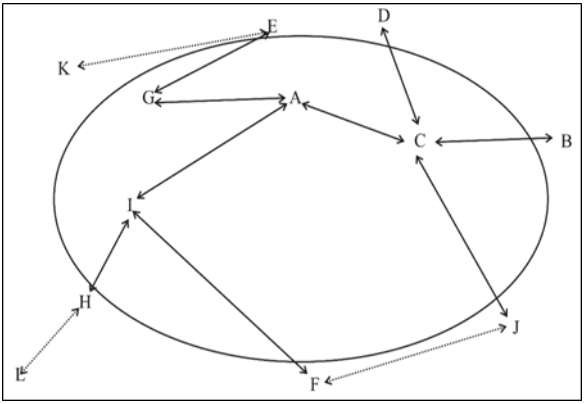

Fig 1.15: A Zone with radius, r=2

1.6 Problems related to routing protocols

The performance issues [36, 37, 38] regarding routing protocols are as follows:

- **Distributed operation:** The route discovery operation is to be carried out by nodes.
- **Loop-freedom:** To save packets for periods of time, the time to live value could be used.
- **Demand based operations:** The route will be established on demand. The drawback will be the longest delay.

- **Proactive operation:** The proactive service will be used because of extra latency occurrence is unacceptable.
- **Security:** It is difficult to maintain the physical security of the media.
- **Sleep period activity:** The mobile nodes can take a pause interval.
- **Unidirectional link support:** As bi-directional links are there, so use of unidirectional links is limited.
- **Network size:** It measures the existence of devices.
- **Network connectivity:** The neighbours connected to a particular node at a time
- **Rate change of topology:** On which speed, the physical arrangement of nodes are updating.
- **Link Power**: The efficiency of a link in bits per second.
- **Presence of one-directional links**: How many unidirectional links are present?
- **Traffic patterns:** The effectiveness property of a protocol for adopting heavy traffic?
- **Mobility:** Which mobility model is the best suitable for specific circumstances?
- **Terminal problems:** There is a problem when two nodes that are hidden from each other send data to same node results in collision of data.

1.7 Mobility models in MANETs

Amongst all other parameters, movements and a pattern of movements play a decisive part in analyzing the achievement of MANET. The pattern on which nodes are moving is designed by the mobility model. The location, angle, and velocity change with time is investigated. During simulation, the selection of mobility model influences the performance of a network [39]. The researchers provided different types of mobility patterns on time to time [40]. They focused on the speed of a device in a specific area at a conceptual level. The initial basic parameters of this level are traffic handling, speed change, and a probability of blocking. Now, researchers are focusing on an atomic level covering coordinates of a device, and a speed of rest of the nodes, because the position of other nodes also affects communication. These models play a vital role in the design of MANET. Simulators like NS, QualNet allow the users to choose the mobility models as these models represent the movements of nodes. Currently there are two types of mobility

models used in simulation study of MANET: traces and synthetic based models. The trace-based model [41] obtains deterministic data from the real system. This mobility model is still in its early stage of research, it is therefore not recommended to be used. The synthetic based model is the imaginative model that uses statistics. In the real world, nodes or objects have their target destination before they decide to move. However, the movement of each mobile node to its destination has a pattern that can be described by a statistical model that expresses the movement behavior in the real environment. This type of mobility model can be either Entity Mobility Model (EMM) or Group Mobility Model (GMM) [42, 43, 44]. In EMM, each node moves independently like Random Waypoint, Random Walk, and Random Direction. For GMM, the movement of each mobile node depends on some other like Column Mobility Model and Reference Point Group Mobility Model. The types of mobility models are depicted in figure 1.16. For some movement patterns, the continuation of a device is dependent on its previous history, known as mobility with temporal dependence. If the set of devices are travelled in a group, then it comes under the category of spatial dependency. In rest of cases, the movements of nodes may interfere by hurdles, and this class deals with mobility models with geographic restrictions. The nodal speed and the average relative speed are the two mobility metrics for each mobility model.

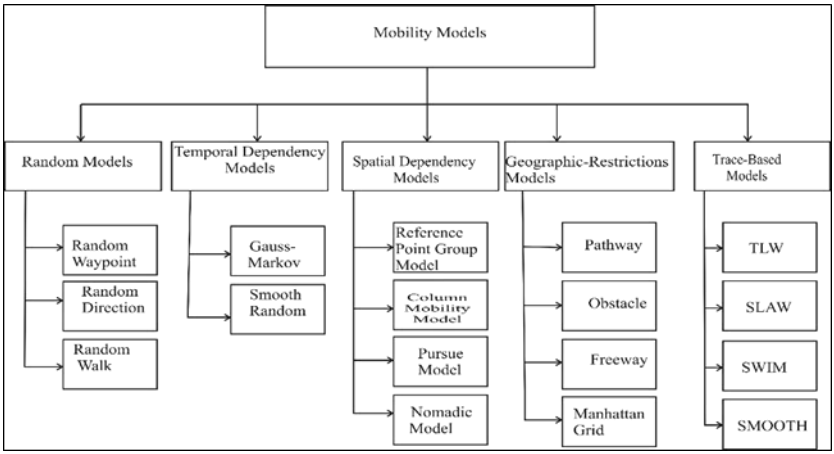

Fig 1.16: Types of Mobility Models [45]

1.7.1 Random-based mobility models

In these mobility models, devices travel freely and independently from any constraints. For all the nodes, the target, velocity, and direction are selected aimlessly and individually from the rest of the devices.

1.7.1.1 The Random Waypoint Model (RWP)

It consists a breathing space interval while modifies its direction along with velocity. After expiring this time of pausing, the mobile nodes choose a random velocity and an independent direction. The chosen speed lies between the maximum and minimum velocity. A mobile node travels with predefined speed in a prescribed way. The same process continues with a break of specified pause interval [46] as shown in figure 1.17.

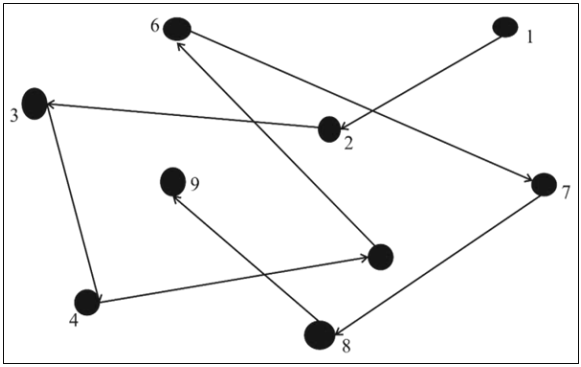

Fig 1.17: Random Waypoint Model

In concern of network simulator NS2, a node chooses its location randomly and moves towards this location with a fixed velocity. This velocity can change from zero to maximum, which is the highest speed. A device takes a pause interval, T_{pause} while reached on the target. A mobile node has a constant velocity with pause time 0. It again chooses a new direction within simulation field and travels in that direction when the pause time is over. The process continues till the simulation ends. The MANET topology based upon RWP will be stable if maximum speed will be small and T_{pause} will be large. It is termed as a nodal speed. A topology will be highly dynamic, if maximum speed will be large and T_{pause} will be small. The average node speed can be calculated as $0.5V_{max}$ if $T_{pause}$is 0. It is defined as the relation of speeds of two nodes [47].

The authors [48] proposed the formula for calculating the relative velocity of two nodes *p* and *r* on time *k* as

$$RS(p,r,k) = \left|\overrightarrow{Vp(k)} - \overrightarrow{Vr(k)}\right| \quad (1.1)$$

A formal definition of calculating the average relative speed of all pairs of nodes and overall time, termed as $\overline{M}$ as follow

$$\overline{M} = \frac{1}{|p,r|}\sum_{p=1}^{N}\sum_{r=p+1}^{N}\frac{1}{T}\int_{0}^{T} RS(p,r,k)dt \quad (1.2)$$

p and r are identifying as a pair, N represents the total nodes, and experiment time is T. The Average Relative Speed can be calculated similarly [49].

1.7.1.2 Random Walk Model (RW)

It is based on the concept of irregular particle movement which is called Brownian motion. Other examples include the path traced by a molecule as it travels in a liquid or a gas, the search path of a foraging animal, the price of a fluctuating stock and the financial status of a gambler: all can be approximated by random walk models, even though they may not be truly random in reality. A device will move to a new direction with a speed from its current location. Every change in the Random Walk happens with constant time, T or a constantly travelled distance, D. Upon termination, a novel speed and direction are measured as shown in figure 1.18. It is a kind of RWP Model with zero break time [50]. The nodes can change the direction and speed at each time break. At break time T, each node randomly and uniformly chooses its new direction $\theta(t)$ from$(0, 2\pi)$. Similarly, the new velocity follows Gaussian distribution from $[0, V_{max}]$. At time break, the node travels with the speed vector $[v(t)\cos\theta(t), v(t)\sin\theta(t)]$. The device bounces back with the angle of $\theta(t)$ or $\pi - \theta(t)$ on reaching the boundary. This property is called the border effect property. It comes under the category of a no-memory model, i.e., present speed is separated from its preceding velocity [50]. As illustrated by those examples, random walks have applications to engineering and many scientific fields including ecology, psychology, computer science, physics, chemistry, biology as well as economics.

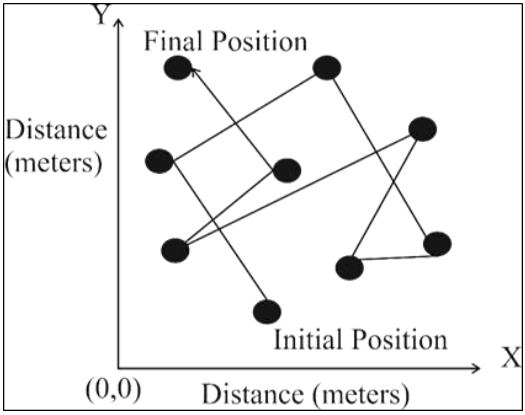

Fig 1.18: Random Walk Model

1.7.1.3 Random Direction Model (RD)

The authors [52, 53] respectively observe property of Random Waypoint model. When the experiment starts, the nodes transforms to non-uniform manner from uniform manner. So, the irregular distribution pattern of devices becomes worse. At the end of the simulation, it reaches a constant state. A maximum number of nodes are lying in the center region, whereas the boundary area is almost empty. This property is called non-uniform spatial distribution. Royer, Melliar-Smith, and Moser [54] observed another phenomenon called density wave phenomenon. According to this, every node has an average number of neighbors, and those are periodically changed along with time. The node distribution of random direction model in rectangular area is shown in figure 1.19. Similarly, spatial node distribution can be maintained by a circular area.

The variation of RWP model is required for uniform spatial node distribution. Based on the similar intuition, the Random Direction (RD) model is invented by Royer, Miller-Smith and Moser [54].

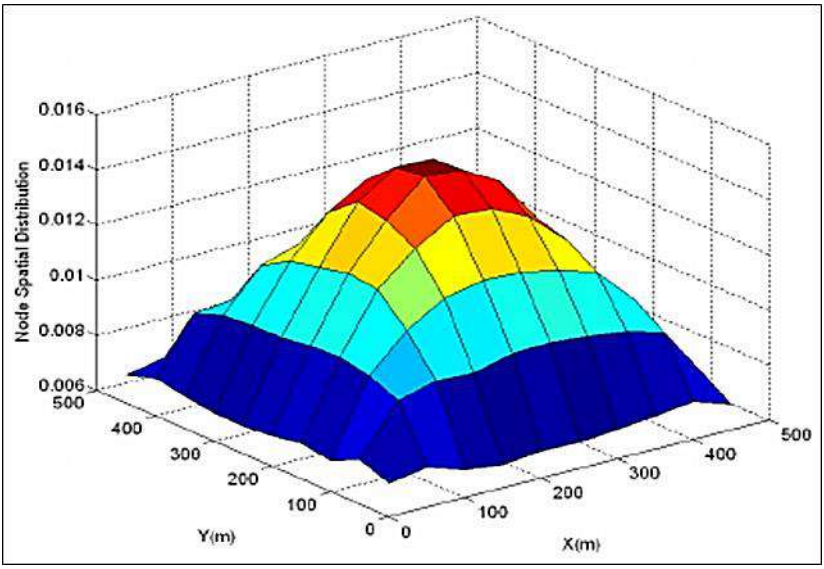

Fig 1.19: Node Spatial Distribution [55]

It resolves the issues of irregular spatial distribution and oscillation issues generated by Random Waypoint model. A device moves randomly to a chosen path and goes to the boundary. It breaks for a specified time T_{pause} upon reaching the boundary. It again chooses a path between 0 to 180 degrees. This action [56] continuously repeats as shown in figure 1.20.

Another form of this model is Altered Random Direction model which gives authority to a device to take pause and select a new direction for going on. This model gives low vibrations in node density than RWP.

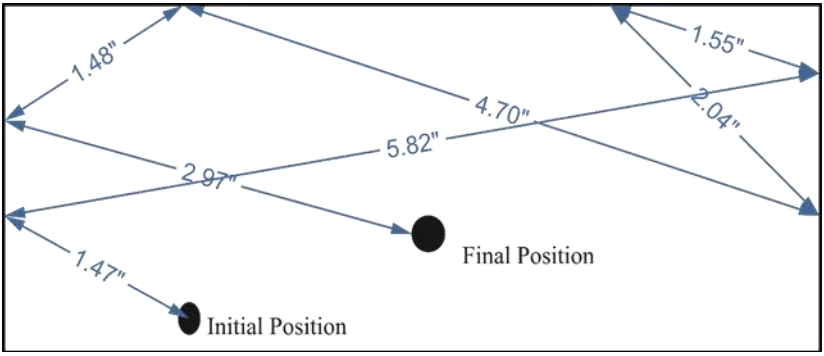

Fig 1.20: Random Direction Model

The above models are universally used due to its simplicity. But it does not hold various dependencies as mobility characteristics. The first limitation is the Temporal Dependency, in which the nature of mobile nodes is memory-less. As traces are created by the RWP model, some mobility events like sudden stop, sharp turn, and sudden acceleration may frequently occur. Many real life scenarios are affected by the speed of vehicles and pedestrians. Despite these, the direction change is also smooth. The second limitation is the Spatial Dependency of Velocity. Every node moves independently as an entity. So these models are categorized as entity model. The third limitation is Geographic Restrictions of Movement. There may be the presence of obstacles, buildings, streets or freeways in reality.

1.7.2 Temporal dependency based mobility models

Node mobility may be limited and constrained by rate of change of direction, velocity, and acceleration. The speed of moving node may depend upon the previous values of speed. So, almost all velocities of moving nodes are 'correlated.'

1.7.2.1 Gauss-Markov Mobility Model (GM)

In this model, a node's speed is calculated on the basis of Gauss-Markov stochastic process [57]. A device has a predefined velocity and direction initially [58]. The node flips to 180 degrees upon reaching the boundary. So, the devices stay away from the boundary of network area. In this temporarily dependent model, the dependency degree is defined by a memory parameter α. The haphazardness of Gauss-Markov process is shown by α. By tuning

this parameter, this model is capable of duplicating different kinds of mobility behaviors in various scenarios. The value of α parameter will be zero in case of memory-less Gauss-Markov. If the Gauss-Markov has strong memory then α will be equal to one. If the Gauss-Markov has some memory then α lies between 0 and 1. Figure 1.21 shows the motion behavior of Gauss-Markov model.

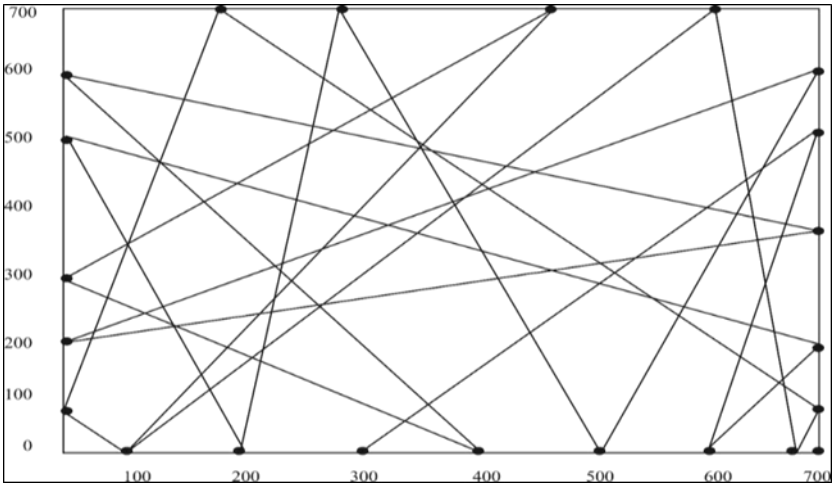

Fig 1.21: Gauss-Markov Mobility Model

1.7.2.2 Smooth Random (SR)

The limitation of RWP is its unnatural and sharp movements which makes it unrealistic. So, Bettstetter [59] proposes a model for smooth movement of the device. The device can move at different speeds $\{V_{pref}^1, V_{pref}^2, V_{pref}^n\}$ instead of the range $[0, V_{max}]$. The probability distribution of speed is the rate of selecting speed of mobile node's choice with higher probability, whereas remaining part of the entire interval is assumed to be uniformly distributed over range $[0, V_{max}]$. The speed change is a Poisson process and when the speed changes, a new velocity $v(t)$ is selected by the rules of probability distribution. The velocity change in Smooth Random mobility model is shown in figure 1.22.

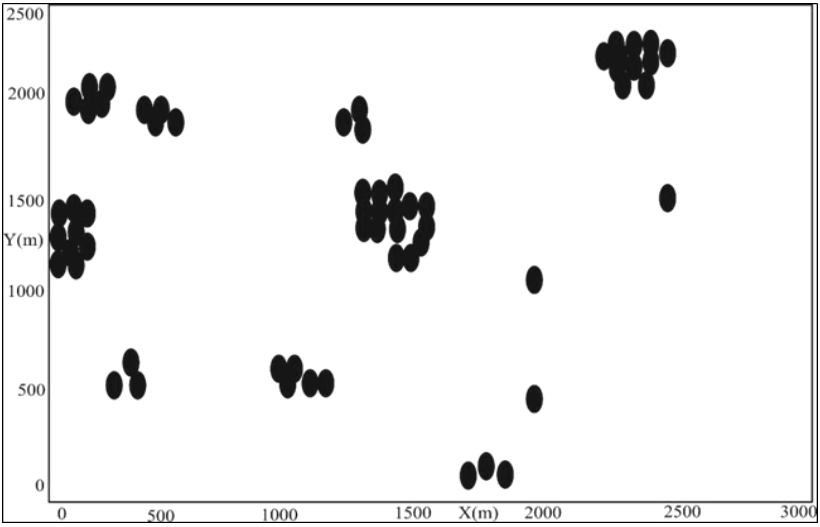

Fig 1.22: Smooth Random Mobility Model

1.7.3 Spatial Dependency Based Mobility Models

The previously discussed models do not hold natural behavior of mobility. Some applications of MANET users like to follow the team leader. The speed of a device could be affected by its next-hops. So, speeds of different nodes are 'correlated' in space which is called Spatial Dependency of speed.

1.7.3.1 Reference Point Group Mobility Model (RPGM)

In MANET, the mobile node tends to coordinate its movement. In RPGM model, the devices go together in a group or platoon and each group has a center, which is either a logical center or group leader node. We assume that the center is the team leader. So, each group has composed of one director and some members. The speed of the group leader determines the mobility behavior of the whole group.

Figure 1.23 presents an abstract of RPGM in which $\overrightarrow{V_{group}^{t}}$ is the motion vector for the group leader and the whole group,$\overrightarrow{RM_i^t}$ is the random deviation vector for group member i. $\overrightarrow{V_i^t}$ represents the final motion vector of group member i.

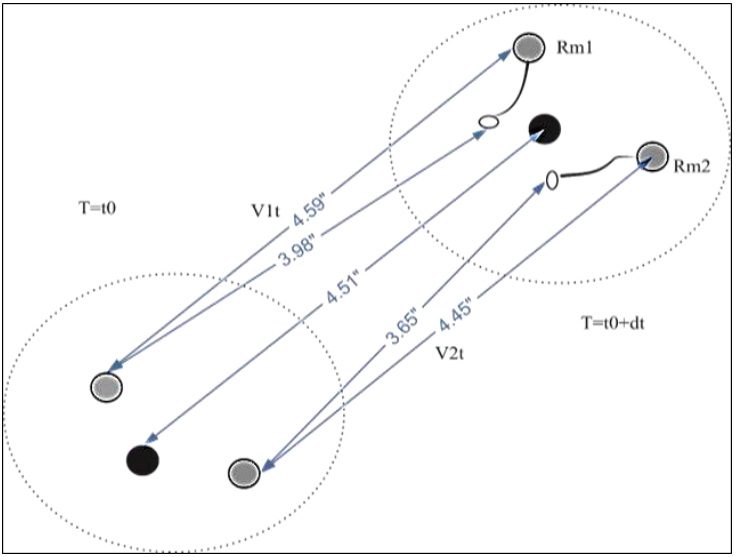

Fig 1.23: Reference Point Group Mobility

It can emulate a variety of mobility behaviors and represent various mobility scenarios including In-Place, Overlap and Convention Models [60].

Hong, Kwon, Gerla *et al*. explored another framework as an enhancement of RPGM [61]. A natural scenario can be created and experimented by wisely choosing the milestones with the proper motion of a group leader. The mobility vector model provides a general and flexible framework for modeling mobility patterns if checkpoints can reflect the motion behavior in realistic scenarios. In general, it is not difficult to create these milestones.

The vector $\overrightarrow{RM_t^t}$ determines the difference between the movement of members and group leader. The speed can be defined as follows:

$$\begin{cases} |V_{member}(t) = |V_{leader}(t)| + random() * SAR * max\_speed| \\ Q_{member}(t) = Q_{leader}(t) + random() * AAR * max\_angle \end{cases} \quad (1.3)$$

Where AAR is the Angle Alteration Ratio < 1, and SAR is the Speed Alteration Ratio > 0. The random motion vector controls the difference of the velocity of group representatives' members from the manager.

1.7.3.2 Column Mobility Model (CMM)

The authors [62] presented a pool of mobility models in which the devices travel collectively. These models are habitual to display high interdependency between the surrounding nodes.

Suppose $P_k^z = (X_k^z, Y_k^z)$ be the exact location of node k at time z and $RP_k^z = (X_k^z, Y_k^z)$ is the reference point.

It presents a collection of mobile devices that travel to a particular fixed way. It is derived from RPGM where the nodes move in scattered way, but in CMM, devices move in one lane. The updated reference point RP_k^z will be:

$$\mathrm{RP_k^z} = \mathrm{RP_k^{z-1}} + \alpha_k^z \quad (1.4)$$

α_k^z is the predefined offset used to move the reference grid of node k at time z. After the reference point is updated, the new position of mobile node k is to randomly deviate from the updated reference point by random vector w_k^z as

$$\mathrm{P_k^z} = \mathrm{RP_k^z} + \mathrm{w_k^z} \quad (1.5)$$

In equation 1.4, reference point has been measured by the advance vector, which is further used in the measurement of finding next position of moving device shown in equation 1.5. The 180 degrees flipping [63] is applicable upon reaching the boundary which is presented in figure 1.24.

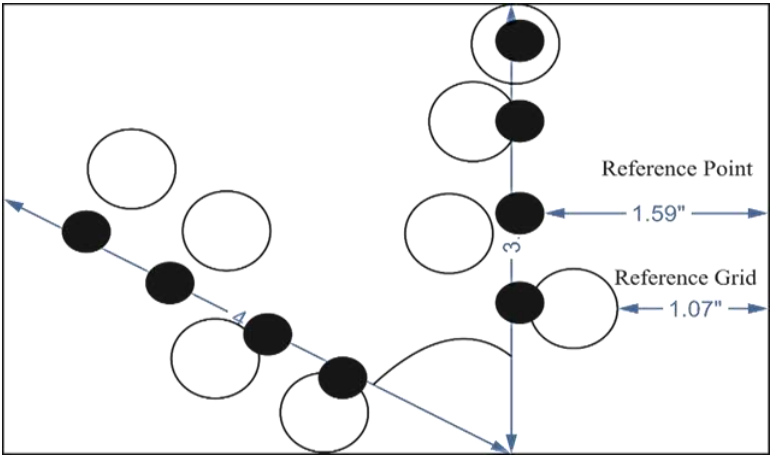

Fig 1.24: Column Mobility Model

1.7.3.3 Pursue Mobility Model (PMM)

The pursue models a group tracking a particular node and presents a pack of nodes attempting to follow an individual target. The current location of a mobile node is obtained by an entity mobility model. Then the current location which is represented by a random point is joined with an expedition function to compute the following status of a node as shown in figure 1.25.

A device travels independently as similar to the Random Waypoint model. It can be formulated as

$$P_i^t = P_i^{t-1} + v_i^t\left(P_{target}^t - P_i^{t-1}\right) + w_i^t \quad (1.6)$$

Where P_{target}^t is the predefined position of the destination device at time *t*, w_i^t is a random point for offsetting, P_i^{t-1} is the previous location, and P_i^t is the current location of a mobile node.

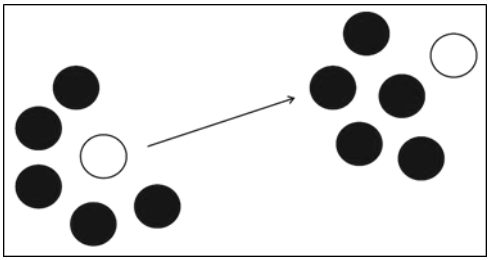

Fig 1.25: Pursue Mobility Model

1.7.3.4 Nomadic Mobility Model (NMM)

In the nomadic group movements, every member has its personal moving space along with individual reference point. This represents a group of devices that travel together. In this, each node in the group follows any entity mobility model to wander around a given point of reference. On the shifting of the reference point, a node may take the new area which is nearby of the reference point and continue moving around this reference point [64] as shown in figure 1.26. The entire group moves randomly and the reference point of an individual node is calculated by the general movement of the group. A random vector is added to the predefined reference point. Formally,

$$P_i^t = RP_i^t + w_i^t \quad (1.7)$$

Where w_i^t is a small random vector used to offset the movement of mobile node *i* at time *t*. It is shown that reference that it shares the same reference grid whereas in CMM each column has its reference point. The movement of nodes in the NMM is sporadic while the movement is more or less constant in CMM model.

The Column, Pursue and Nomadic mobility models behave differently than Random Waypoint model.

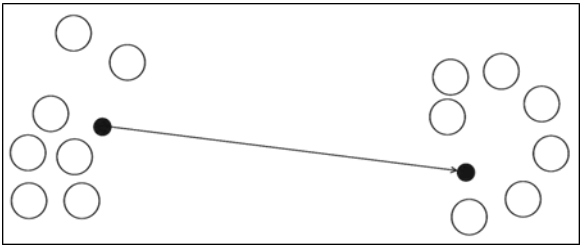

Fig 1.26: Nomadic Mobility Model

1.7.4 Mobility models with geographic restrictions

In natural scenarios, a node has the freedom to travel randomly. In urban areas, the movements are restricted to lanes and streets. So, movement of nodes must be predicted manner on the specified pathway. Such type is called a geographically restricted mobility model.

1.7.4.1 Pathway Mobility Model (PWM)

To express natural obstacles into the mobility model, a pathway can be designed on the map. This map will be predefined in the Network area. A non-uniform graph is designed to model the city map which is predefined in the network area. The buildings are presented as vertices, and streets and freeways are depicted as edges.

$$G = (V, E) \tag{1.8}$$

On the edges of the graph, mobile nodes are placed. A destiny is chosen randomly by a node and node which will go to the target by the short length path. The node will take rest for a time upon reaching the target which is known as pause time and then chooses the next destiny. It continues until the simulation ends. A device can travel to the lanes only. A pseudo-random fashion is opted by the nodes for traveling which is presented in figure 1.27 [57].

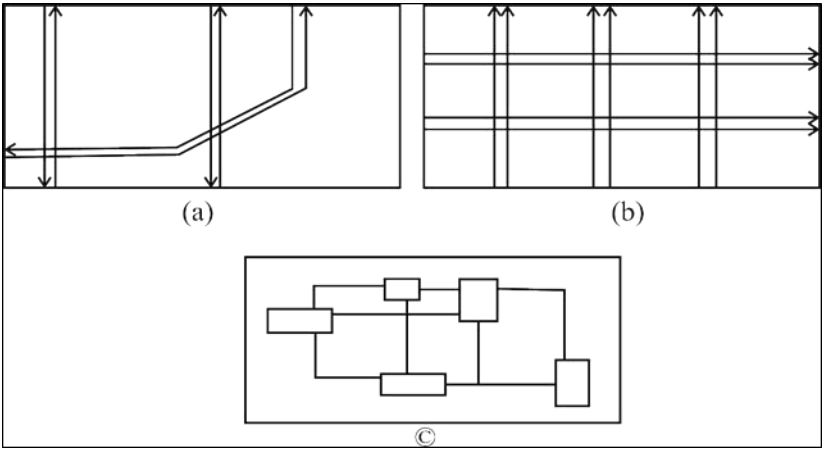

Fig 1.27: (a) Freeway, (b) Manhattan, and (c) Pathway Mobility Models

1.7.4.2 Obstacle Mobility Model (OSM)

Because geographic content plays a significant impact in movement patterns, there may be the provision of obstacles existing in the simulation field. If obstacles come in the path of moving the node, the node has to modify its direction. It also affects the speed of moving vehicles. In a similar example of radio propagation, radio signals behave well in the outdoor environment and behave poorly with some attenuation in the outdoor environment. The researchers proposed following scenarios as per real life:

1) In a scenario of conference holding 50 persons, some people have with very little mobility and most of them are static.
2) In Event coverage scenario consists of highly mobile vehicles and people which change their positions very frequently.
3) In Disaster relief scenarios consists of fast moving nodes and slowly moving nodes.

Obstacles are placed in the form of rectangular boxes in random fashion manner on the simulation field. A proper movement trajectory is chosen by the mobile node. A signal is absorbed by the barrier completely on the radio signal propagation. The authors also investigated the effect of constraints on modelling mobility. A vehicle movement is clearly shown in figure 1.28 without trajectories and propagation of radio signals. They analyzed the movement of people on predefined paths between buildings rather than random movements.

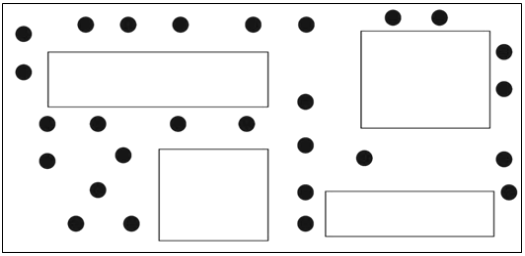

Fig 1.28: Obstacle Mobility Model

A graph, named as Voronoi graph is designed to draw the lanes. The lanes connect the buildings and a device can travel on these lanes only. A vehicle can enter or exit out from buildings. The vehicle movement is strictly restricted to the defined pathway. A node travels to the target by getting the short length path. The process of finding the minimum length path is done by Dijkstra algorithm.

1.7.4.3 Freeway Model (FWM)

This model imitates the movement nature of devices on a Freeway. This model is used frequently while changing the status of traffic and checking the status of an individual vehicle. For this purpose, it takes help of maps and follows a directed graph in shape as given in figure 1.29. A number of freeways are plotted on a map which handles traffic in both directions. A vehicle is bounded to its lane only and every vehicle has the impact of temporal dependence. For solving the situation of accidents on the same lane, a Security Measure (SM) is always maintained. The velocity of the succeeding vehicle cannot exceed the speed of its predecessor vehicle.

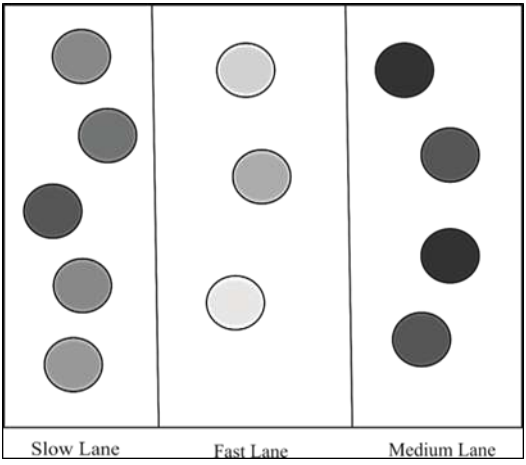

Fig 1.29: Movements in Freeway Model

1.7.4.4 Manhattan Grid (MG)

The Manhattan model has the same restrictions on the speed of the freeway model as shown in figure 1.27. However, in this case, nodes can change directions at the intersections with probability p=0.5 to stay on the same street and equal probability of p=0.25 to turn left or right.

1.7.5 Trace-based mobility models

These models are known as real dataset models. The datasets are collected from various internal/external sites available on CRAWDAD which is one of huge database for real traces. These datasets are possessed from various scenarios. The traces are totally dependent upon the scenarios for which they were collected. A real dataset results cannot be applicable for another dataset. Traces can be collected by locations, and contact information.

1.7.5.1 Truncated Levy Walk (TLW)

This model uses the dataset in the form of traces which are generated from five outdoor sites by Global Positioning System (GPS). It includes Disney World, two campuses, a metro city scenario, and a state fair. To remove any kind of interruption like noise, the traces are already pre-processes. The traces are acted as refiners to remove the noises which may be present in the pattern of movements. For the very first time, nodes are scattered non-uniformly in the Network as depicted in figure 1.30. A device may take power-law jumps for random directions. It rests for a specified pause time after reaching to the site as presented in figure 1.31.

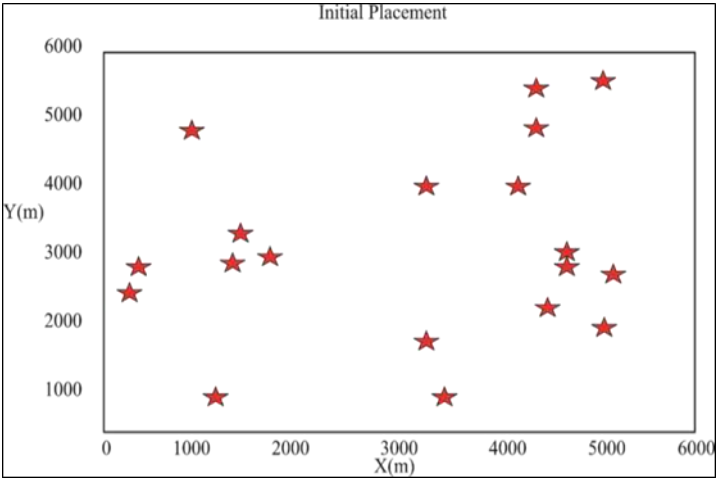

Fig 1.30: Startup TLW

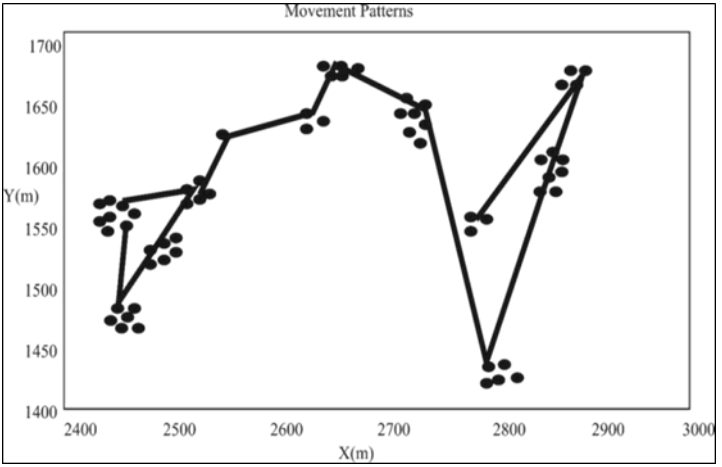

Fig 1.31: TLW Movements

1.7.5.2 Self-Similar Least Action Walk (SLAW)

It collects the same set of traces as used in TLW model. The locations are also captured as similar processes. If the aggregated processes are highly correlated then a process is called self-similar. A Hurst parameter controlled the distribution of locations, which can be varied from 0.5 to 1. A node may travel for the scenario with Hurst parameter=0.75 for the initial distribution of locations. The value estimation for the Hurst parameter is quite difficult. For this purpose, different Hurst estimators are used to provide multiple values. The startup distribution of devices and their movement methods are shown in figure 1.32 and figure 1.33 respectively.

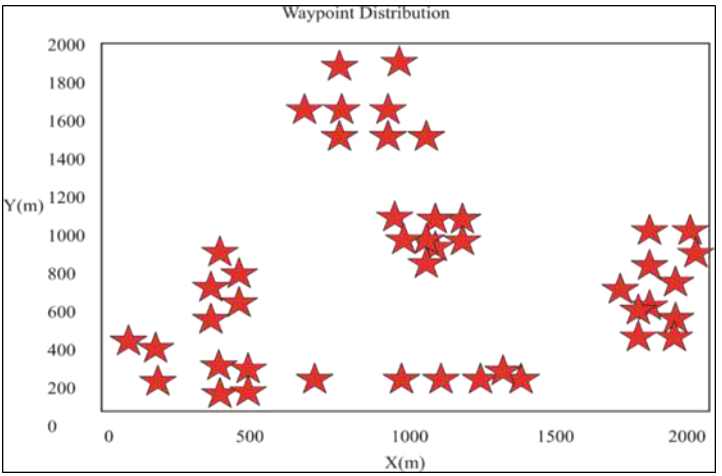

Fig 1.32: SLAW Startup

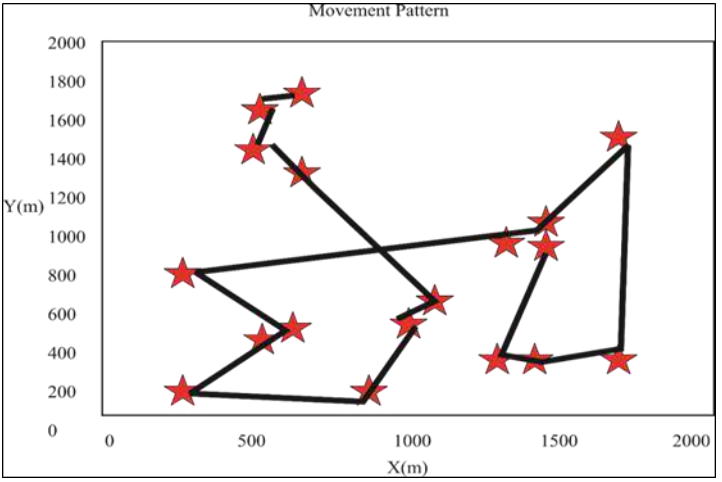

Fig 1.33: SLAW Movements

1.7.5.3 Small World In Motion (SWIM)

This mobility model follows the two intuitions of human action: how far the location is, and how accessible the site is. In this model, nodes travel areas on the basis of distance and popularity of this location. The scenario is the collection of equally divided areas called cells. Every node exists in its home cell. A target cell is selected by the home node on basis of its distance and popularity. One input variable is dedicated for decision, denoted as μ. If μ is closer to 1, a node will travel to nearer location from its home site; if μ is closer to 0, a mobile node prefers to visit famous cells in the network. Figure 1.34 shows the template of movement with μ=0.25.

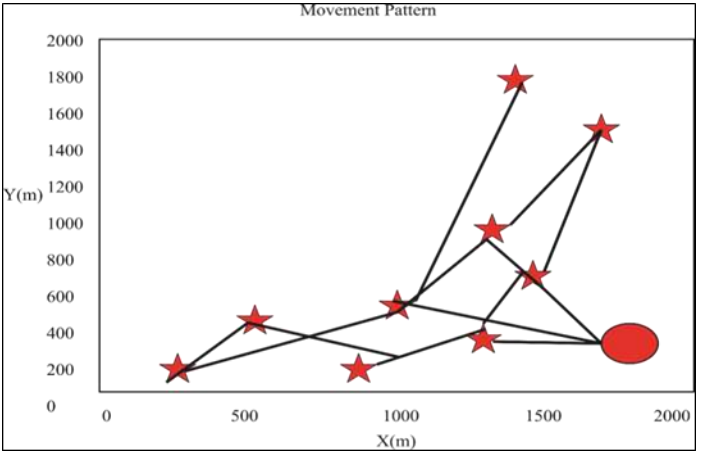

Fig 1.34: Pattern of movement with μ =0.25

1.7.5.4 SMOOTH

In a novel model called SMOOTH, the popular locations are placed as landmarks in the starting of the network. These locations are indicated as landmark locations. A mobile node can revisit the previously visited locations with a already defined probability. Figure 1.35 and figure 1.36 shows the visited sites by mobile nodes.

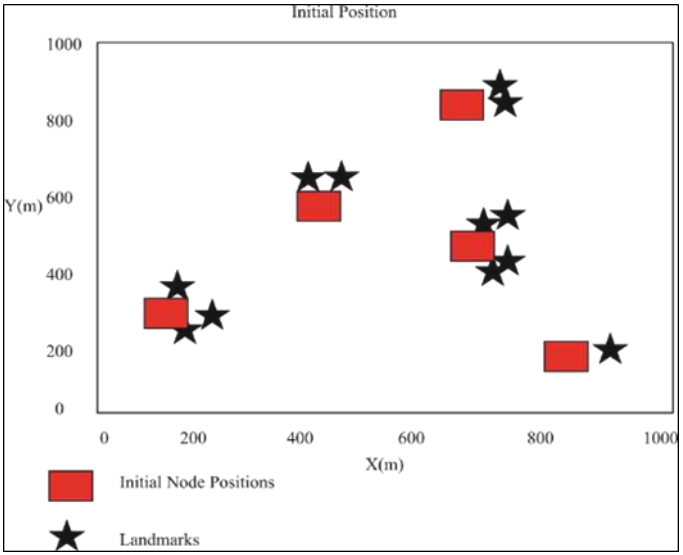

Fig 1.35: SMOOTH Initial Positions

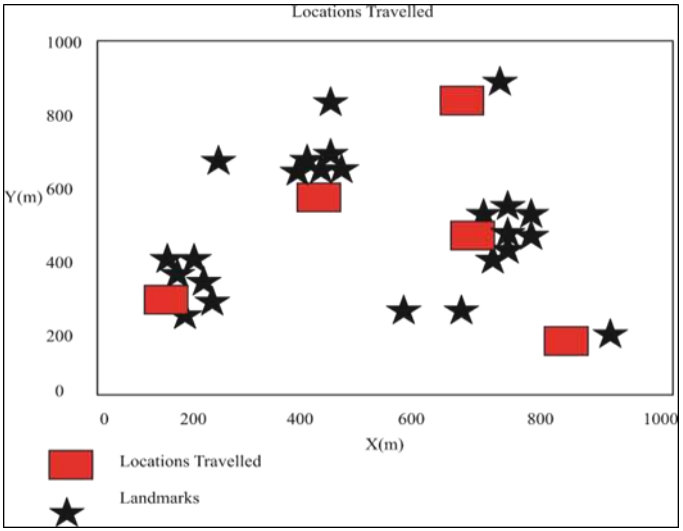

Fig 1.36: Locations Visited in SMOOTH

1.8 Mobility metrics

The mobility model is classified into two types of mobility metrics - direct and derived. The speed, relative speed comes under the category of direct mobility metrics. It concerns about the actual movement of a mobile node. The graph connectivity falls under derived mobility metric. It concerns about the mathematical modeling of physical speed of mobile node. The classification of mobility models has been carried out based on mobility metrics taking into account of above two categories and tabulated in Table 1.1.

Table 1.1: Mobility Metrics

Sr. No.	Metrics	Metric Class	Characteristics	Mobility Model
1.	Direct Mobility	Random Based	No dependencies, restricted model	RWP, RW, RD, Cluster in
		Temporal Dependence	Previous movements involved	GM, SR
		Spatial Dependence	Node's movement influenced by surrounding nodes	RPGM, CMM, NMM, PMM
		Geographical Restrictions	Node movement restricted in particular geographical area	Graph-based, Geographic Division based, Map-based, Voronoi-based
2.	Derived Mobility	Hybrid Structure	Combination of all mobility metrics	FW, MG
		User-Oriented with three components	Provide a Modeling approach for complex mobility scenario-spatial environment, observation based, temporal and spatial dependencies	Tactical scenario like Catastrophe scenario, platoon, Disaster-area model

The Direct mobility metrics is an independent protocol metrics, and its attempt is to explore the mobility behavior characteristics among the mobile nodes. It directly calculates the host movement like average host speed. The average relative speed, temporal dependency and spatial dependency are other metrics of direct mobility metrics. It covers relative speed, and average relative speed, temporal dependence degree, average of temporal dependence degree, spatial dependence degree, and average of spatial dependence degree [42].

The derived mobility metrics capture properties, theoretic models for graph and mathematical modeling. The impact of speed can be analyzed by the connected graph showing connectivity between the mobile nodes. It covers total links, changing of links, and average of changing links, duration of link, average duration of link, available path, and average availability of paths [42].

1.9 Summary

This chapter reflects overview to MANETs, uses, and characteristics followed by discussion about issues in performance of MANET. A brief introduction to MANETs is provided and how they differ from wired networks was given. The outline to the problems related to wireless communication is highlighted. An elaborated description of routing protocols is given; their path discovery process and path maintenance procedures are described. The mobility models are also explained with mobility metrics.

References

1. Rappaport TS, Gibson JD. Wireless Communications: Principles and Practice and the Mobile Communications Handbook. IEEE, 1998.
2. O'Hara B, Petrick A. The IEEE 802.11 Handbook: A Designer's Companion. IEEE Press, New York, 1999.
3. https://www.researchgate.net/figure/Conventional-cellular-network-with-fixed infrastructure -a-and-mobile-ad-hoc-network_fig4_277930076.
4. Corson S, Macker J. Mobile Ad hoc Networking (MANET): Routing Protocol Performance Issues and Evaluation Considerations. RFC 2501, 1999, 1-12.
5. Zhou L, Haas ZJ. Securing ad hoc networks. IEEE Network, 1999, 24-30.
6. http://www.rfidc.com/docs/introductiontowireless_standards.htm.
7. Ramanathan R, Redi J. A Brief Overview of Ad Hoc Networks: Challenges and Directions. IEEE Communication Magazine. 2002;40(5):20-22.
8. Wang F, Zhang Y. Improving TCP performance over Mobile Ad Hoc Networks with Out-Of-Order Detection and Response. Proc. IEEE/ACM MobiHoc'02. 2002, Lausanne, 217-225.

9. Chalmtac I, Conti M, Liu JJN. Mobile ad hoc networking: Imperatives and Challenges. Ad Hoc Networks. 2003;1(1):13-64.

10. Nahian S, Tervonen J. Semi-infrastructure mobile ad-hoc mesh networking. Proc. 14th IEEE Proceedings on Personal, Indoor and Mobile Radio Communications, 2003, 1069-1073.

11. Xie Z, Wang J, Zheng Y, Chen S. A novel anycast routing algorithm in MANET. Proc. IEEE Pacific Rim Conference on Communications Computers and Signal Processing (PACRIM 2003), 2003, 314-317.

12. Latiff LA, Fisal N. Routing protocols in wireless ad hoc network-a review. Proc. 9th Asia-Pacific Conference on Communications, 2003, 600-604.

13. Hsu J, Bhatia S, Takai M, Bagrodia R, Acriche MJ. Performance of mobile ad hoc networking routing protocols in realistic scenarios. IEEE Military Communications Conference, 2003, 1268-1273.

14. Yu D, Li H. On the definition of ad hoc network connectivity. Proc. International Conference on Communication Technology Proceedings, 2003.

15. Radha S, Shanmugavel S. Implementation of node transition probability based routing algorithm for MANET and performance analysis using different mobility models. Journal of Communications and Networks. 2003;5(3):202-214.

16. Sanchez M. Mobility Models. http://www/disca.upv.es/misan/mobmodel.htm, 2003.

17. Jardosh A, Blending-Royer EM, Almeroth KC, Suri S. Towards Realistic Mobility Models for Mobile Ad hoc Networks. Proc. International Conference on Mobile Computing and Networking (MobiCom'03), 2003, 217-219.

18. Camp T, Boleng J, Davies V. A Survey of Mobility Models for Ad Hoc Network Research. Wireless Communication and Mobile Computing (WCMC): Special Issue on Mobile Ad Hoc Networking: Research, Trends and Appl. 2002;2(5):483-502.

19. Chayabejara A, Zabir SMS, Shiratori N. An enhancement of the IEEE 802.11 MAC for multihop ad hoc networks. Proc. IEEE 58th Vehicular Technology Conference, 2003, 3020-3024.

20. Wu K, Harms J. Multipath routing for mobile ad hoc networks. Journal of Communication and Network. 2002;4(1):48-58.

21. https://en.wikipedia.org/wiki/Wireless_ad_hoc_network.

22. Vaughan-Nichols SJ. Mobile IPv6 and the future of wireless Internet access. Computer. 2003;36(2):18-20.

23. Mark JW, Weihua Z. Wireless Communications and Networking, Prentice Hall, 2003.

24. Bai F, Sadagopan N, Helmy A. Important: A Framework to Systematically Analyze the Impact of Mobility on Performance of Routing Protocols for ad hoc networks. Proc. IEEE Information Communication Conference (INFOCOM 2003), 2003, 825-835.

25. https://www.researchgate.net/figure/Classification-of-Ad-hoc-Routing-Protocols_fig1_49592757.

26. Pirzada AA, Portmann M, Indulska J. Performance Comparison of Multi-Path AODV and DSR Protocols in Hybrid Mesh Networks. Proc. IEEE International Conference on Networks, 2003, 587-592.

27. Chi L, Hao Z, Yao C, Zhang Y, Wang K, Sun Y *et al*. A Simulation and Research of Routing Protocol for Ad hoc Mobile Networks. Proc. IEEE International Conference on Information Acquisition, 2006, 16-21.

28. Thorup RE. Implementing and evaluating the DYMO routing protocol. Thesis, M. Tech. University of Aarhus, Denmark, 2007.

29. Fang G, Yuan L, Qingshun Z, Chunli L. Simulation and Analysis for the Performance of the Mobile Ad Hoc Network Routing Protocols. Proc. 8th International Conference on Electronic Measurement and Instruments, 2007, 571-575.

30. Bo SM, Xiao H, Adereti A, Malcolm JA, Christianson B. A Performance Comparison of Wireless Ad Hoc Network Routing Protocols under Security Attack. Proc. Third International Symposium on Information Assurance and Security, 2007, 50-55.

31. Divecha B, Abraham A, Grosan C, Sanyal S. Analysis of Dynamic Source Routing and Destination-Sequenced Distance-Vector Protocols for Different Mobility Models. Proc. First Asia International Conference on Modelling & Simulation, 2007, 1-6.

32. Abusalah L, Khokhar A, Guizani M. A survey of secure mobile Ad Hoc routing protocols. IEEE Communications & Tutorials. 2008;10(4):78-93.

33. Mahfoudh S, Minet P. An Energy Efficient Routing Based on OLSR in Wireless Ad Hoc and Sensor Networks. Proc. 22nd International Conference on Advanced Information Networking and Applications-Workshops, 2008, 1253-1259.

34. Lakhtaria KI, Patel P. Analyzing Zone Routing Protocol in MANET Applying Authentic Parameter. Global Journal of Computer and Technology. 2010;10(4):114-118.

35. Ishrat Z. Security issues, challenges & solution in MANET. International Journal of Computer Science & Technology. 2011;2(4):108-112.

36. Goyal P, Parmar V, Rishi R. MANET: Vulnerabilities, Challenges, Attacks, Application. International Journal of Computational Engineering & Management. 2011;11:32-37.

37. Vijaya I, Rath AK, Mishra PB. Influence of Routing Protocols in Performance of Wireless Mobile Adhoc Network. Proc. Second International Conference on Emerging Applications of Information Technology, 2011, 340-344.

38. Roy RR. Mobility Models Characteristics. Handbook of Mobile Ad hoc Networks for Mobility Models, Springer, Boston, 2011, 23.

39. Maan F, Mazhar N. MANET Routing Protocols vs. Mobility Models: A Performance Evaluation. Proc. Third International Conference on Ubiquitous and Future Networks (ICUFN), 2011, 179-184.

40. NCSU Networking Research Lab. Human mobility models download, 2011.

41. Pamportes S, Tomasik J, Veque V. A Composite Mobility Model for Ad Hoc Networks in Disaster Areas. REV Journal on Electronics and Communications. 2011;1(1):62-68.

42. Bai F, Helmy A. Ä Survey of Mobility Models in Wireless Adhoc Networks, 2008. http://www.cise.ufl.edu/~helmy/papers/Survey-Mobility-Chapter-1.pdf. 1-30.

43. https://en.wikipedia.org/wiki/Mobility_model.

44. https://www.semanticscholar.org/paper/Performance-Evaluation-of-VANET-with-EDC A-Access-P.H-Perdana/04642b8820200509da9bd7b4aeaa547f55d9f9d9/figure/2.

45. https://en.wikipedia.org/wiki/Random_waypoint_model.

46. Bettstetter C, Hartenstein H, Perez-Costa X. Stochastic Properties of the Random Waypoint Mobility Model. ACM/Kluwer Networks, Special issue on Modeling and Analysis of Mobile Network. 2004;10(5):555-567.

47. Johansson P, Larsson T, Hedman N, Mielczarek B, Degermark M. Scenario-based performance analysis of routing protocols for mobile ad-hoc networks. Proc. International Conference on Mobile Computing and Networking (MobiCom'99), 1999, 195-206.

48. Ikeda M, Kulla E, Hiyama M, Barolli L, Takizawa M. Analysis of MANET routing protocols in Indoor Environment. Proc. International Conference on Broadband, Wireless Computing, Communication and Applications, 2010, 9-16.

49. Tie-yuan L, Liang C, Tianlong G. Analyzing the Impact of Entity Mobility Models on the Performance of Routing Protocols in the MANET. Proc. Third International Conference on Genetic and Evolutionary Computing, 2009, 56-59.

50. https://en.wikipedia.org/wiki/Random_walk.

51. Bettstetter C. Mobility Modeling in Wireless Networks: Categorization, Smooth Movement and Border Effects. ACM Mobile Computing and Communication Review. 2001;5(3):55-67.

52. Bettstetter C, Wagner C. The Spatial Node Distribution of the Random Waypoint Mobility Model. Proc. German Workshop on Mobile Ad-Hoc Networks (WMAN), 2002, 41-58.

53. Royer EM, Melliar-Smith PM, Moser LE. An Analysis of the Optimum Node Density for Ad hoc mobile networks. Proc. IEEE International Conference on Communications (ICC), 2001, 857-861.

54. https://www.researchgate.net/figure/3-Node-Spatial-Distribution-Square-Area_fig3_250745075.

55. Atsan E, Ozkasap O. A Classification and Performance Comparison of Mobility Models for Ad Hoc Networks. The Scientific and Technical Research Council of Turkey, 2006, 444-457.

56. Aschenbruck N, Gerhards-Padilla E, Martini P. A survey on mobility models for performance analysis in tactical mobile networks. Journal of Telecommunication and Information Technology. 2008;2:54-61.

57. Ariyakhajorn J, Wannawilai P, Sathitwiriyawong C. A Comparative Study of Random Waypoint and Gauss-Markov Mobility Models in the

Performance Evaluation of MANET. Proc. International Symposium on Communications and Information Technologies, 2006, 894-899.

58. Zhao M, Wang W. Design and Applications of a Smooth Mobility Model for Mobile Ad Hoc Networks. Proc. 2006 IEEE Military Communications Conference, 2006, 1-7.
59. Bettstetter C. Smooth is better than Sharp: A Random Mobility Model for Simulation of Wireless Networks. Proc. ACM International Workshop on Modeling, Analysis, and Simulation of Wireless and Mobile Systems (MSWiM), 2001.
60. Hong X, Gerla M, Pei G, Chiang CC. A Group Mobility Model for Ad Hoc Wireless Networks. Proc. ACM International Workshop on Modeling and Simulation of Wireless and Mobile Systems (MSWiM), 1999, 53-60.
61. Sichitiu ML. Mobility Models for Ad Hoc Networks. Computer Communications and Networks, 2009, 237.
62. Sanchez M, Manzoni P. A Java-based Ad Hoc Network Simulator. Future Generation Computer System. 1999;17:573-583.
63. Kaur S, Ubhi JS. Analysis of scalability for AODV routing protocol under CMM in Mobile Adhoc Networks. Proc. International Conference on Latest Developments in Material, Manufacturing & Quality Control, 2016, 612-616.

Chapter - 2
Performance of Cascaded Asymmetric Multilevel Inverter using Double Source Cell

Authors

P. Sarala
Assoc. Professor, Dept. of EEE, Malla Reddy Engineering College, Hyderabad, Telangana, India

M. Dilip Kumar
Assoc. Professor, Dept. of EEE, St Peters Engineering College, Hyderabad, Telangana, India

Chapter - 2

Performance of Cascaded Asymmetric Multilevel Inverter using Double Source Cell

P. Sarala and M. Dilip Kumar

Abstract

The growth of Power Electronic industry is focused towards the development of new power devices, higher rated switches and reduced blocking voltages for the desired operations to cater the needs of domestic and other industrial sectors especially in the field of variable frequency and variable voltage applications. The appropriate choice is the power modulators and emphasises to continue exploring alternatives The Phase Disposition Pulse Width Modulation strategy is utilized to generate control input of the switches and ensure the desired operation of the power modules. It follows to bring in modified topology based on twin source cells to extract a variable amplitude output voltage with the theory of fundamental switching using optimal switching angle control. The optimised angles are derived using Galactic Swarm Optimisation (GSO) technique. The effort is further carried to derive the optimal structures of the proposed topology based on different optimisation parameters like maximisation of levels and minimisation of switches. The study propels with MATLAB based simulation and experimental results obtained using dSPACE controller DS1104 / Cyclone IV E FPGA for the appropriate prototypes to illustrate the viability of the proposed concepts. The promising nature of the presentation, expands the insight of utilizing the MLIs for sustainable power source related applications.

Keywords: MLI, PWM, MLI structure

1. Introduction

AC power supply with variable amplitude at fixed frequency or variable frequency is obtained through one of the ways, by converting DC power using Inverter power circuits. DC power can be acquired using renewable energy sources or by using uncontrolled rectifier / controlled rectifier which is based on the regenerating capacity at the load side. As per the

requirement, the Inverter circuit is configured in singlephase or three-phase. The single-phase inverter output (Colak *et al*., 2011; Rodriguez *et al*., 2002) is a square wave with 48% Total Harmonic Distortion (THD) operated at the fundamental frequency. To improve the THD level, passive types of filters are utilized. Another way of improving THD of single-phase inverter is by operating the inverter switches at high frequency under different switching scheme namely unipolar, bipolar,.., etc. Though the THD is improved, to meet the Power demand, three-phase inverter is preferred and the output voltage waveform called quasi square gives better THD compared to single-phase square inverter. To claim a further reduction in THD under three-phase, the above single-phase switching schemes are extended to three-phase and additional passive filter circuits are also used. Three-phase inverter finds extensive application in industry (Kazmierkowski *et al*., 2011). The thesis is concentrated on single-phase configuration

Multilevel inverter originates output voltage waveform in a staircase with equal amplitude nearer to sinusoidal in shape through isolated dc sources, dc-link capacitors, CD (clamping diodes) and FC (flying capacitors)(Garc´ıa Franquelo *et al*., 2008). The increase in the number of levels forges the inverter output voltage nearly sinusoidal shape resulting in high-quality waveform while the count of dc sources and conducting switches tend to increase. Due to control flexibility, CHBMLI is further explored in the direction of unequal DC sources aiming at higher levels with a reduction in the number of devices. Though four switching devices are used for every additional DC source, the number of conducting switch is also increased. Several remarkable topologies in cascaded type have been reported to foresight the above drawbacks (Samsami *et al*., 2017; Elias *et al*., 2014; Babaei *et al*., 2013). The topology of (Babaei, Laali and Alilu, 2014) requires 6 switches for every additional pair of DC sources and nine algorithms for determining the source magnitude is highlighted. Prototype for 49-level is developed using the best suggested algorithm. The structure presented in (Jayabalan *et al*., 2017), uses bidirectional switch and for every addition of DC source, one bidirectional switch is needed to complete the circuit MLI continues to provide space for utilizing energy through a power converter interface with improved power quality. The advancement of multilevel inverter topologies has more perspective in adjustable speed control drives, power quality and utility applications (Rodriguez *et al*., 2002)

2. Proposed topology using double source cell

Using basic cells namely double source cell and auxiliary cell, the proposed topology is framed. The basic auxiliary cell ‘Ac’of Fig. 4.1a

constitute one DC source ‘Va’with complementary auxiliary switches (Sa and S a). The other basic cell DSC shown in Fig. 4.1b is composed of double dc sources (Vd and V d), two bidirectional switch (Sp, Spp) and two unidirectional switch (Sd,Sy). The corresponding switches of DSC are controlled to connect the double sources to the load. By connecting ‘nd’ number of DSC in series, the proposed MLI topology is constructed to synthesise even number of levels at the output with upper and lower half bridge structure switches (S1, S2) and (S 1,S 2) respectively under even structure configuration termed as even structure DSC MLI(ESDSCMLI) and shown in Fig.. By the addition of Ac to ESDSCMLI, another topology called as odd structure double source cell MLI(OSDSCMLI) is derived and is projected in Fig.. Hence, DSCMLI is classified into ESDSCMLI and OSDSCMLI.

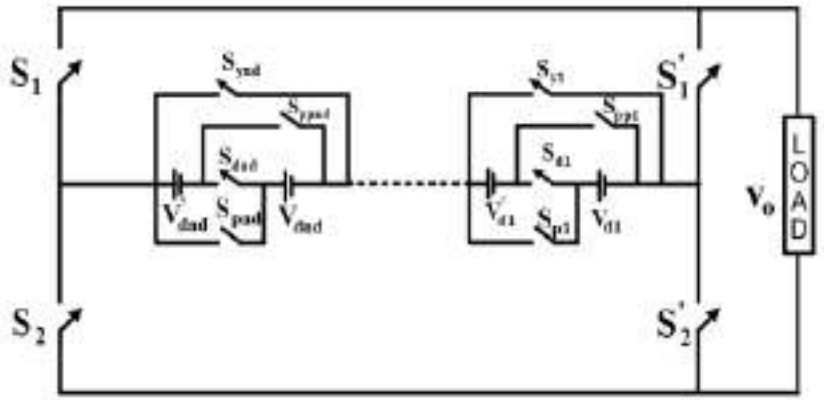

Fig 2.1: Generalized proposed topology of ESDSCMLI

The topology under symmetric mode(all sources with equal Vdc) with odd/even (ns) number of DC sources, the ’m’ number of output levels of the odd/even structure MLI module is given by m=2ns+1. The corresponding number of DSC for OSDSCMLI with odd number of ns(≥ 3) is nd = (ns-1)/2, are connected in series with Ac. With even number of ns(> 2), the required DSC for ESDSCMLI is nd = (ns − 2)/2 are cascaded. Under symmetrical mode, with ns=4, nd=2, m=9, the number of switches ‘sw’ is 12 and only 4 switches are turned on to get all the levels and the different switches are subjected to different blocking voltages Whereas for CHBMLI, sw is 16 and 8 switches are switched on to get every level and the blocking voltage is same for all the switches. Though the proposed DSCMLI in symmetric mode has redundant states compared to CHBMLI, the efficiency is more and few switches are in conduction path. For better utilisation, the

proposed topology is configured in asymmetric mode for synthesising higher number of levels with reduced count and PDPWM switching scheme is used.

2.1 Types of source magnitude algorithm under asymmetric mode

With the availability of high voltage switching devices, the proposed topology DSCMLI is operated in asymmetric mode with the following source voltage magnitude algorithms for generating different levels and the TNDS is derived for all the algorithms for generating the required level.

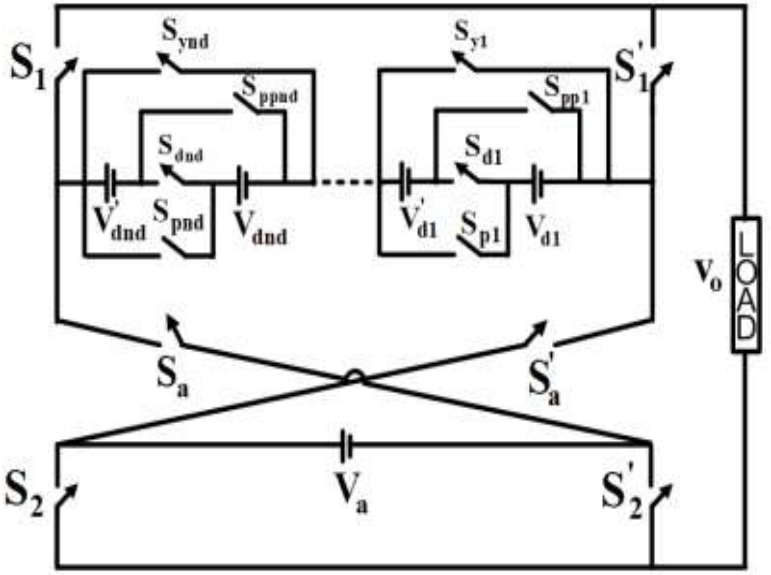

Fig 2.2: Generalized proposed topology of OSDSCMLI

Besides, the number of conducting switches against each algorithm is also derived and the Table illustrates the relation between the number of sources and levels for each algorithm.

The different algorithms are:

- Type 1 algorithm (1 : 2)×Vdc
- Type 2 algorithm (1 : 2 : 2) : (5 : 5 : 15 : 15 : ...)×Vdc
- Type 3 algorithm (1 : 2 : 2) : (6 : 6 : 18 : 18 : ...)×Vdc
- Type 4 algorithm (1 : 2 : 3 : 4 : 5...)×Vdc
- Type 5 algorithm (1 : 2) : (2 : 4 : 8 : ..)×Vdc
- Type 6 algorithm (1 : 2) : (3 : 6 : 9 : .. :)×Vdc
- Type 7 algorithm (1 : 2 : 4 : 8 : ..2ns−1)×Vdc.

Table 2.1: Relation between ns and 'm 'for the proposed source magnitude algorithms

Algorithm type	n_s
Type 1	$0.25m+0.25$
Type 2	even source : $2\left(\frac{\ln(0.45m-0.45)}{\ln 3}\right)$ odd source : $2\left(\frac{\ln(0.1\times 3^{(\frac{3}{2})})(m-1)}{\ln 3}\right)$
Type 3	even source : $2\left(\frac{\ln(0.375m+0.375)}{\ln 3}\right)$ odd source : $2\left(\frac{\ln(0.25m+0.25)}{\ln 3}\right)$
Type 4	$0.5\sqrt{4m-3}-1$
Type 5	$\sqrt{0.5m-3.25}+0.75$
Type 6	$\frac{\left(\sqrt{9+\frac{4}{3}(m-13)}\right)+3}{2}$
Type 7	$\left(\frac{\ln(0.5m+0.5)}{\ln 2}\right)$

3. Non-conventional symmetric and asymmetric MLI topologies

The non-conventional MLI topologies or novel topologies are derived as per the Fig. 3.1 and also with the help of novel cell structures. The recent topologies (symmetric and asymmetric types) available in the literature are reviewed. The topology suggested in comprises of a combination of three-level (3L) active neutral-point-clamped inverter and floating capacitor connected parallel to the legs of H-bridge. Two switches operated at fundamental frequency are connected across the DC link structure and enhances the topology performance by a two-fold increase in RMS value. Through logical mapping, the switches are turned on /off by deriving the pulses through voltage balancing scheme and the scheme balances the floating capacitor voltage regardless of load angle. Cascading five-level diode clamped MLI with seven level or 9 level conventional Cascaded H

Bridge (CHB) Multilevel Inverters (MLI) results in hybrid topology for generating 11-level 13-level respectively. The conventional MLI has a case to case merits and demerits. In the presented topology, the demerits of the conventional topology are minimized by cascading two different conventional topologies. The proposed MLI switches at the fundamental frequency and the operation is shown for a particular modulation index and variable load angle.

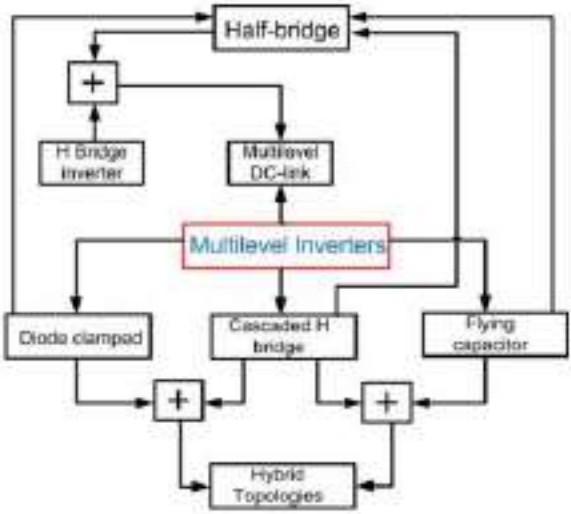

Fig 3.1: Capacitor balancing is attained between the charging cycle and the recharging cycle. A new symmetric structure for cascade multilevel converter is developed in which is composed of several series-connected switched capacitor diode units and an H-Bridge inverter for polarity reversal. A fewer number of device count is required for configuring the topology. Besides, optimal structures derived from the proposed topology projects the merits by maximizing the number of levels with different objectives such as a minimum number of switch count and sources. The simulation and experimental results added to show the performance of the proposed method and the results are compared with other structures.

3.1 Cascaded asymmetric multilevel inverter

The advancement of multilevel inverter topologies has more perspective in adjustable speed control drives, power quality and utility applications (Rodriguez *et al*., 2002). Multilevel inverter originates output voltage waveform in a staircase with equal amplitude nearer to sinusoidal in shape through isolated dc sources, dc-link capacitors, CD (clamping diodes) and FC (flying capacitors) (Garc´ıa Franquelo *et al*., 2008). The increase in the number of levels forges the inverter output voltage nearly sinusoidal shape

resulting in high-quality waveform while the count of dc sources and conducting switches tend to increase. Due to control flexibility, CHBMLI is further explored in the direction of unequal DC sources aiming at higher levels with a reduction in the number of devices. Though four switching devices are used for every additional DC source, the number of conducting switch is also increased. Several remarkable topologies in cascaded type have been reported to foresight the above drawbacks (Samsami *et al*., 2017; Elias *et al*., 2014; Babaei *et al*., 2013). The topology of (Babaei, Laali and Alilu, 2014) requires 6 switches for every additional pair of DC sources and nine algorithms for determining the source magnitude is highlighted. Prototype for 49-level is developed using the best suggested algorithm. The structure presented in (Jayabalan *et al*., 2017), uses bidirectional switch and for every addition of DC source, one bidirectional switch is needed to complete the circuit

4. Proposed EMC and other recent multilevel converter topologies

In this section recent multilevel converter topologies with reduced number of switches and total blocking voltages are taken into account. In Fig. (a), the number of switches against number of levels is shown. In that, requires higher number of switches than conventional topologies. The CHB MLC configure in both symmetric and asymmetric method. Since the proposed topology is symmetric, the CHB symmetric is considered. It is clear that proposed topology and require lower number of switches than the other topologies. The symmetric configuration is considered for the comparative analysis because the proposed EMC is suitable for symmetric method not asymmetric method. The cost of the multilevel converter presented is depends on the factors like the number of switches, diodes, capacitors and sources as given.

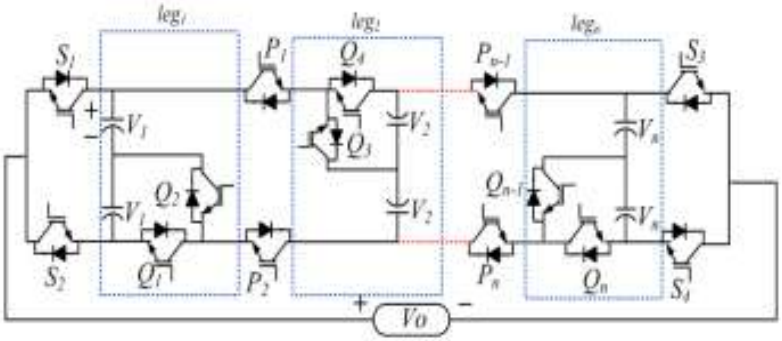

Fig 4.1: Proposed Extended Multilevel Converter (Emc) Topology

5. Simulation and results

To verify the performance of proposed extended multilevel converter is simulated and tested for 13-level as shown in fig.5.1. The nearest level modulation (NLM) technique is used to generate the switching. The NLM technique operates in fundamental switching frequency which reduces the switching losses. This 13-level converter consists of three dc sources, six capacitors and 14 switches. Each capacitor rating is 1000µf/ 35V for both the simulation and hardware.

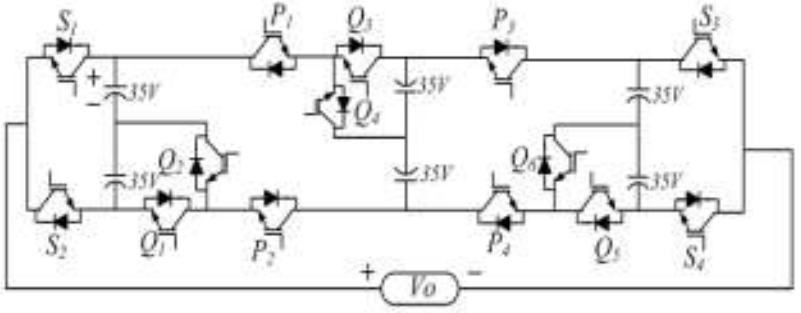

Fig 5.1: Test System

The switches P1, P2, P3 &P4 have a maximum voltage of 105V. The output power 448 Watts is observed across the R-L load with value of 35Ω &100mH. The load is highly inductive which gives the power factor of 0.73. In Fig. 5.2 (a) and (b) shows the simulated steady-state load voltage, current waveforms and FFT spectrum, respectively. The maximum output voltage.

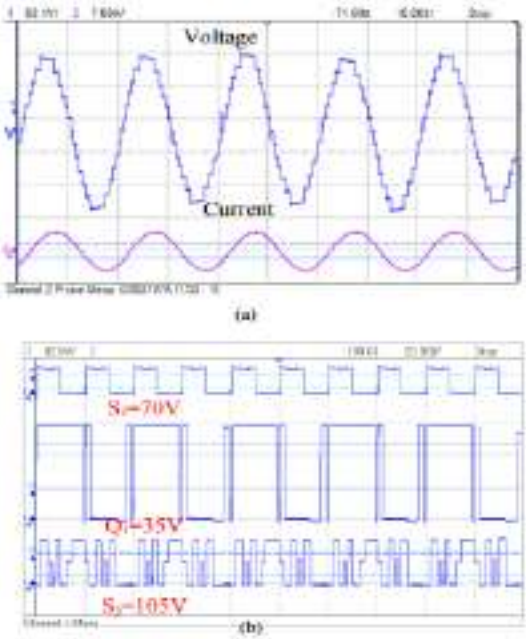

Fig 5.2: (A) Experimental Output Voltage and Current Waveform (B) Blocking Voltage across the Switches (S1, Q1 And S3).

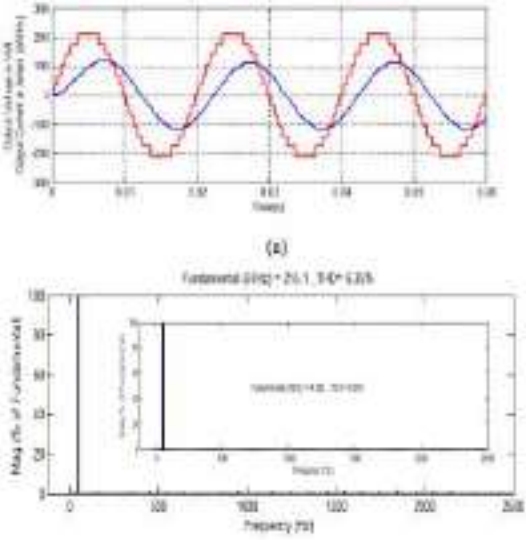

Fig 5.3: (a) Simulation output voltage and current waveform (b) Corresponding voltage and Current FFT analysis results

Conclusion and future scope

Conclusion

The proposed converter can produce any level at output voltage waveform. The required mathematical results were provided for calculating the value of blocked voltage on switches. The proposed topology is a suitable candidate in PV applications. The comparison results were proven that the proposed topology has lower blocked voltage on switches compared to the other topologies. Also, it was shown that the proposed multilevel converter requires the least number of power switches compared to conventional topologies. The simulation and experimental results were verified and confirmed the performance of the proposed multilevel converter.

Future scope

The capacitor helps boost the number of levels through various combinations by a factor of 1.5 in symmetric mode and a factor of 1.6 in asymmetric DC combinations. The performance of the topology is proved to be satisfactory in static as well as in dynamic conditions. Experimental validation is done using the developed prototype. The promising results are obtained in the experimental setup. The topology is compared with other topologies to confirm the effectiveness and assert that the topology is suitable for the various medium- and high-power applications

References

1. Babaei E, Hosseini SH. New cascaded multilevel inverter topology with minimum number of switches. Energy Conversion and Management. 2009;50(11):2761-2767.
2. Kangarlu MF, Babaei E. A Generalized Cascaded Multilevel Inverter Using Series Connection of Submultilevel Inverters, IEEE Trans. Power. Electron. 2013;28(2):625-636.
3. Shalchi Alishah R, Nazarpour D, Hosseini SH, Sabahi M. Reduction of Power Electronic Elements in Multilevel Converters Using a New Cascade Structure, IEEE Trans. Ind. Electron. 2015;62(1):256-269.
4. Alishah RS, Hosseini SH, Babaei E, Sabahi M. Optimal Design of New Cascaded Switch-Ladder Multilevel Inverter Structure, IEEE Trans. Ind. Electron. 2017;64(3):2072-2080.
5. Ebrahimi J, Babaei E, Gharehpetian GB. A New Multilevel Converter Topology with Reduced Number of Power Electronic Components, IEEE Trans. Ind. Electron. 2012;59(2):655-667.

6. Ebrahimi J, Babaei E, Gharehpetian GB. A New Topology of Cascaded Multilevel Converters with Reduced Number of Components for High-Voltage Applications, IEEE Trans. Power Electron. 2011;26(11):3109-3118.

7. Babaei E, Laali S, Bahravar S. A New Cascaded Multilevel Inverter Topology with Reduced Number of Components and Charge Balance Control Methods Capabilities, Electric Power Components and Systems. 2015;43(19):2116-2130.

8. Babaei E, Laali S, Alilu S. Cascaded Multilevel Inverter With Series Connection of Novel H-Bridge Basic Units, IEEE Trans. Ind. Electron. 2014;61(12):6664-6671.

9. Mokhberdoran A, Ajami A. Symmetric and Asymmetric Design and Implementation of New Cascaded Multilevel Inverter Topology, IEEE Trans. Power Electron. 2014;29(12):6712-6724.

Chapter - 3
Fatehpur Sikri: A City Frozen in Time

Authors

Gunjan
Assistant Professor, School of Architecture and Planning,
Lovely Professional University, Phagwara, Punjab, India

Jimmy Gupta
Assistant Professor, School of Architecture and Planning,
Lovely Professional University, Phagwara, Punjab, India

Chapter - 3

Fatehpur Sikri: A City Frozen in Time

Gunjan and Jimmy Gupta

Abstract

India is a country which is full of historic monuments. One of them is Fatehpur Sikri which is one of the of the World's Heritage Site. Fatehpur Sikri (City of Victory), constructed by Emperor Akbar in the second half of the sixteenth century, served as the capital of the Mughal Empire for around ten years. The Jama Masjid, one of India's largest mosques, is part of the complex of monuments and temples, all of which share a consistent architectural style. It is a magnificent site which was deserted just after few years of use as the capital of Mughal Empire. Moreover the site is famous for its architectute and planning details which they considered while designed which needs to thoroughly studied and examined to get the useful lessons which can be used by the planners and architects of today. This book chapter is an attempt to criticize the planning concepts and principles used to plan Fatehpur Sikri and also study the infrastructure planning details of the city.

Keywords: Akbar, Fatehpur Sikri, spatial planning, mughal planning, mandala.

Introduction

Fatehpur Sikri, known for its architecture and planning, is a world heritage monument. It was commissioned by a Mughal Emperor Akbar and was completed in less than 15 years (1569-1574). Fatehpur Sikri served as the capital of Mughal Empire for a very short time from 1569-1585. At present most of its buildings are in excellent condition. It is city frozen in time. Fatehpur Sikri is located 37 km from Agra. Since the area is close to the western desert region, the climate is hot-dry with relatively little rainfall.

The main source of information about Fatehpur Sikri is Akbar Nama by Abul Fazal. Even the travelogues of British travellers give us a lot of information (Shaukat Mahmood, 2017).

Historical evolution

Fatehpur Sikri was generally significant since it was on this site Babur, the granddad of Akbar took on and won a conflict against Rajasthani ruler, Rana Sanga of Mewar. To commend his triumph, Babur spread out a nursery which is visited by all the Mughal rulers (Ali, 2014).

Akbar's choice to move his capital from Agra to Fatehpur Sikri depended on close to home reasons. It was done on the grounds that Fatehpur Sikri was home of Sufi holy person, Salim Chisti, who announced that Akbar would clearly have a child and after that Akbar's better half got pregnant with his first kid (Singh, 1995).

National and Regional background

It was not at all important from the strategic point. This city evolved because it was the residence of Salim Chisti. The city was located 22 miles from Agra and 120 miles from Delhi, both of which were very important cities of that time. It was also a part of royal corridor which was 300 mile long from Agra to Ajmer. Fatehpur Sikri was located in between these two cities and act as a link between Agra and Ajmer which is a well-known spiritual centre.

Local background

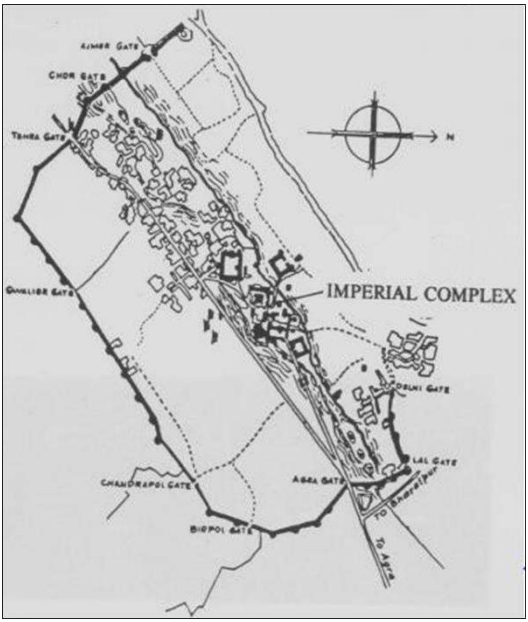

Fig 1: Showing walled city of Fatehpur Sikri with its 9 gates

Fatehpur Sikri is surrounded by walls on 3 sides and on the fourth side by the river Yamuna. There are 9 entrance gates in the outer wall as shown in Figure 1. There were two main purpose of this wall. It define the limits of the city as well as works as defense to protect from outer invasions.

Population and Society

To get to know about the population and social distribution of the city under Akbar, travelogues of a lot of European travellors were studied as there was little knowledge about the same in Akbar Nama. Ralph Fitch, a well-known British traveller, wrote that Fatehpur Sikri was a city larger than London in population. Hence it can be derived that it had population more than 2 lakhs because the population of London in 16^{th} century was around 1.5 lakh to 2 lakh. Moreover he also said that the people of this city were very poor and lived in mud and thatch roof houses. There was a division in society. Poor people were working as servants to wealthy class. The rich were people used to live around the river whereas the poor away from the river. Most of these houses of poor people did not withstand the harshness of climate and the structures which are present today are those of royal family.

Pre-existing structures

There were two structures available before Akbar made it the capital city. They were:

i) Salim Chisti's monastery.

ii) Caravanserai: On the outer edges of Imperial Complex.

That's the reason why the style and colour of stone used in the construction of Caravanserai is different from that used in Imperial Complex. Grey stone is used in its construction whereas red sandstone in other parts.

Moreover Salim Chisti's monastery comprises of a mosque which was used by him and the town people and was known as stone cutters mosque.

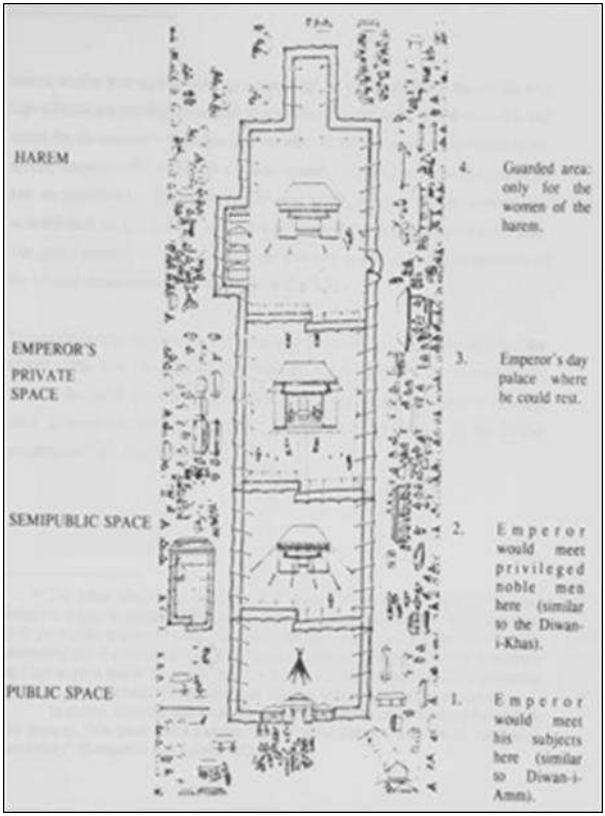

Fig 2: Map of Mughal Encampment by Attilio Petriciolli

Planning Concepts of Mughal Encampment as criteria of the Fatehpur Sikri Plan

It has been speculated by the historians that the plan of Fatehpur Sikri is inspired by Naksha-i-Ain-Manzil, which is actually the plan of Mughal encampment. As we know that the king Akbar travelled a lot both for religious and political reason and every time they made a stop the camp was made in a particular fashion. That particular arrangement was painted by Attilio Petriciolli on a cloth which is shown in the figure. The camp was arranged in a linear fashion and is based on the principle of public and private spaces as described in the figure 2.

It also follows the concept of masculine and feminine spaces which was very famous amongst Islam. The first three spaces can be described as masculine and the fourth one as feminine. Hence comparing the two figures (Figure 2 and Figure 3) in a nutshell we can say that the planning of

Fatehpur Sikri is done on the basis of land use (functional) and flexibility of Mughal encampment.

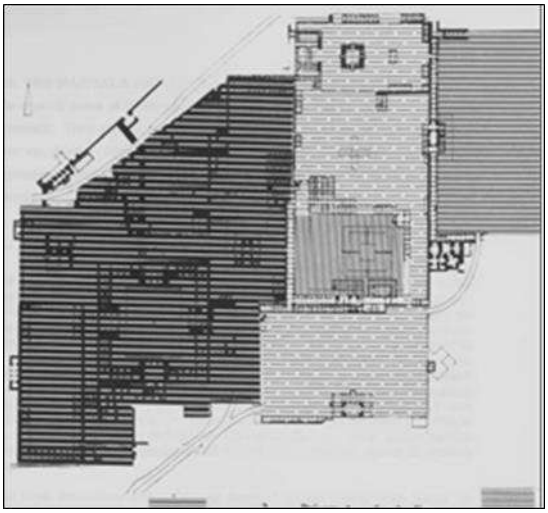

Fig 3: Fatehpur Sikri Plan in terms of Mughal encampment

Planning Principles

The plan of Fatehpur Sikri is very open, flexible and carefree. It was basically designed on Akbar's ideology of Din-e Ilahi. It reflects democracy. It welcomed all the citizens from all religions and considered them as one. During the reign of Akbar, a new relation between the king and its subjects was created which was based on trust and fairness especially with the ones who were not Muslims. This relationship in particular along with geographical features formed the base point of planning of this capital city of Fatehpur Sikri.

Orientation and Skillful organization of the terrain

According to Prof. R. Nath, the buildings were divided into three different parts (Figure 4 and because the ridge did not have even level and terraces for each type of complex were made.

- Sahn-i-Ibadat (The Sacred Complex).
- Sahne-i-Khas (The Royal Complex).
- Sahn-i-Rayyat (The Public Court).

This organization was according to the social stratification in which royal people were placed little higher than common people.

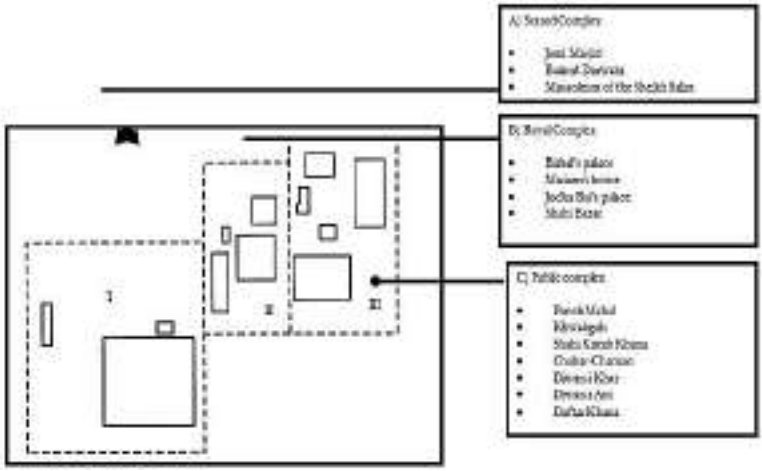

Fig 4: Orientation of the three complexes of Fatehpur Sikri

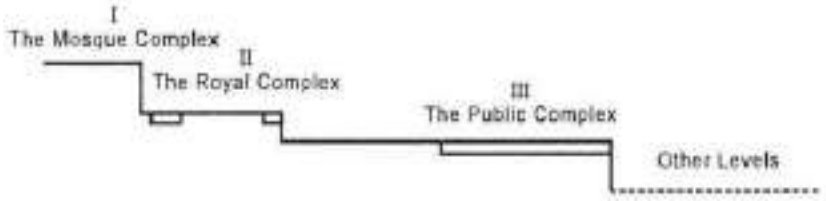

Fig 5: Terraced Sectional Planning of Fatehpur Sikri

The orientation of the buildings on all three terraces is on N-S axis of the ridge, facilitating them to either face east or north (Figure 6 and 7).

Fig 6: North South elevation of the complex

Fig 7: East West elevation of the complex

Symmetry, Multiple Axes and Grid System

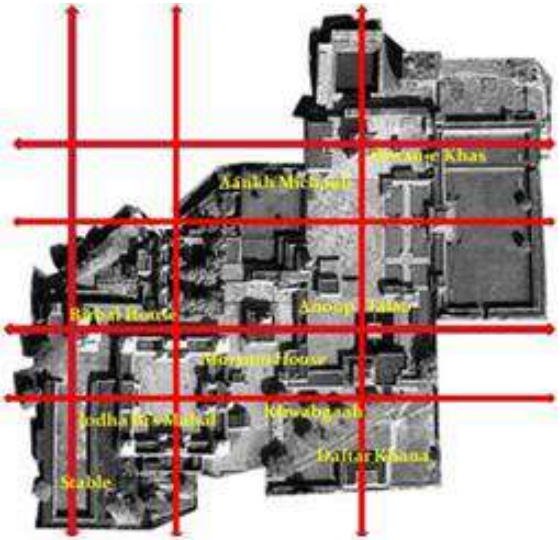

Fig 8: Plan highlighting multiple axes

At first glance the plan of Akbar's City looks very irregular but when studied and analyzed precisely one can find an order in its planning which is done following the principle of multiple axes. If we look closely one can find that the whole planning of Fatehpur Sikri was done in main 3 vertical axes and 4 horizontal axes (Figure 8).

The entire royal complex is divided into eight squares and these eight squares are further divided into 9 sub squares. These squares formed the 29 squares which forms the grid of the whole complex around which it is planned. All the main buildings of the complex is interconnected through courtyards and cloisters which are positioned according to the grid system as explained above parallel to the great mosque.

Another criteria used for planning of city was private, semi private and public buildings. The planning was done in concentric circles keeping the private areas like Harem in the centre, semi private around it and public activity areas and amenities in the exterior.

Mandala and Mughal Planning

There are a lot of speculations that the planning of Fatehpur Sikri is based on Mandala Planning system of Hindus because under Akbar mandala in the form of nine square grid is used in a lot buildings, gardens and tombs like Agra Fort. But mandala was not used in the grid planning of Fatehpur

Sikri as done in Jaipur. Moreover the plan of Fatehpur Sikri does not follow any other town plan given by the Hindus under Mansaras. (Nath, 2000)

This is because of the reason that Akbar wanted to build this city in more flexible terms without following any rigid rules.

Drainage and Water Supply

Drainage

Drains and reservoirs were planned in advance before actual construction of the building can take place. Provision of water is a very primary necessity and the architect has taken care of that (Peck, 2014).

The mosque complex

- The rain water of the mosque complex was drained into several tanks and reservoirs.
- A stone masonry tank, measuring 8.68 m square side and 1.22 m in depth, it was originally more than 6.10 m deep to contain water for the whole year.
- It was also a large reservoir capable of containing the water for the year (Figure 9).

Fig 9: Jhalra Storage Tank

The royal complex

- The Royal Complex has a drainage system, beginning from the roof gargoyles to underground drains, but it does not have a reservoir.
- The red sandstone Char Chamand tank also called Anup Talao is square in plan, 29.26 m side (Figure 10).
- In its middle is a beautiful island platform 9.14 m square with jali balustrade and a raised seat 3.96 m square.

The public complex

- Drainage water from the Public court and also the surplus water of the Anup Talao tank was further diverted to the tank situated.
- It was a deep tank with capacity to supply water the year round.

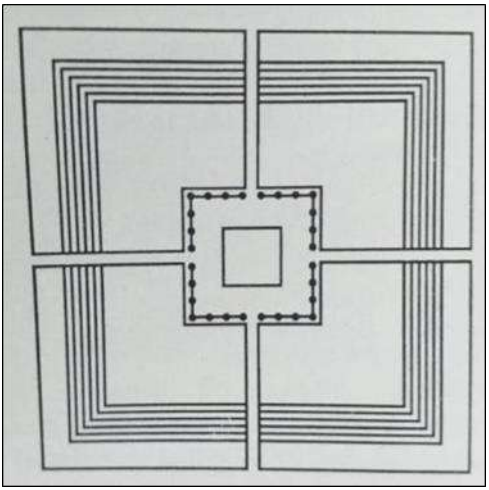

Fig 10: Plan of Anup Talao

- It is an extremely deep storage tank with a comfortable flight of steps and a big underground drain, serving as inlet, on one side (Figure 11).
- It is a rubble construction which should have been originally plastered over.

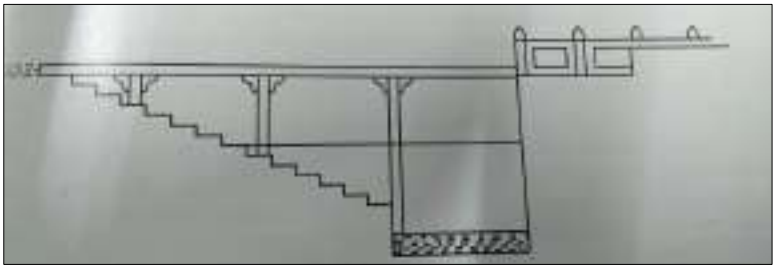

Fig 11: Section of Anup Talao

Water supply

Despite the fact that the waste arrangement of the complex was productive and expand however developers of Fatehpur Sikri didn't rely upon it completely and furnished royal residences on the edge with two

expound water works one on its either side to guarantee the inventory of crisp and clean water. These water were located as follows:

- The first one was on the elephant gate which is still there (Figure 12).
- The other one was sangin baoli (original source of perennial water) near Hiran Minar

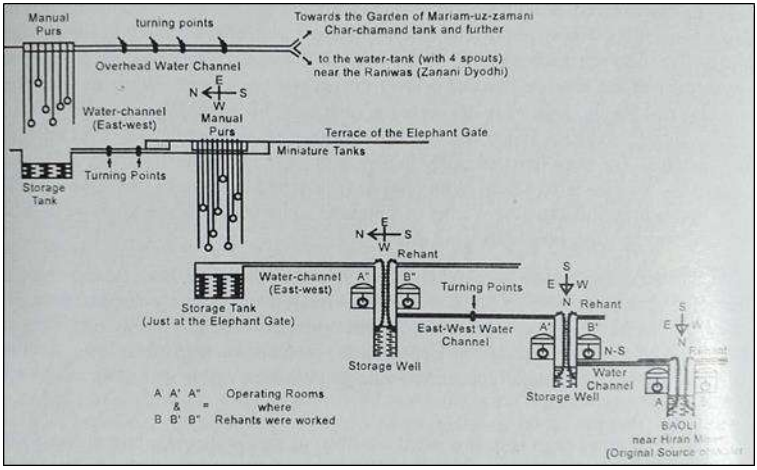

Fig 12: Water Supply System, Elephant Gat

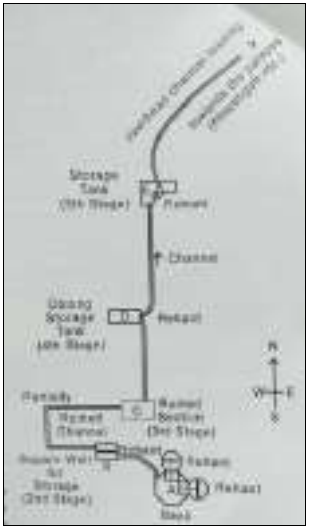

Fig 13: Water Supply System, S-E side

An effective arrangement of rehants, channels, wells and tanks, courses and reservoir conduits (Figure 13) was advanced to convey water starting with one spot then onto the next, from the most reduced level to the most elevated and a steady supply of water was kept up in the castles and hammams consistently (Koch, 2013).

A stone well, likewise with normal enduring wellspring of water provided water to Khass-Hammam and other connecting royal residences on this side of the edge, this was worked out in an a lot littler scale.

Rain water harvesting system

The rain water system of Fatehpur Sikri is one of the oldest one which is properly documented.

Flow of rain water

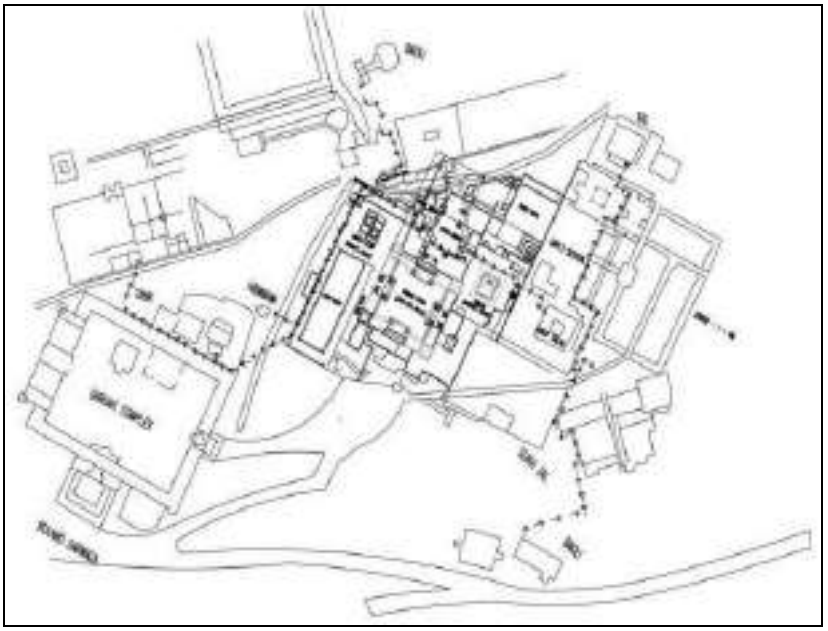

Fig 14: Rain Water supplied to Tal in Public Complex

The rain water falling on the roof falls on the plinth of the particular building. From the plinth the water either enters the surface drains which were covered at few spaces only or they used to enter the holes on the other side of platform and then enter the drain (Figure 14). These drains then take the water either of the tank for use. Extra water of the complex is flowed into Kundas through cascades which were small in size. The size was small because Mughals liked to hear the voice of falling water. The collected rain

water was used by the common people or in public complex works (Koch, 2013). The rain water collected is constantly diverted to public complex first to Anup Talao tank and then to the one situated to the north of Diwan-I Khas. When the water was surplex in Royal Complex then it is diverted to Anup Talao tank. The tank were also made of Red Sandstone.

Cause of decline

Akbar, an ambitious conqueror and restless traveller was not a man to stay at one place. He stayed at Fatehpur Sikri for fourteen years and then in 1585 he left for Punjab and never came back. Later on the city was abandoned by its citizens too and it became a ghost town. (Sharma, 2008)

The reason for this abandonment of the city that Akbar has built with so much enthusiasm is a mystery till now and no one is able to give correct reason with facts. But there has been a few theories regarding it. They are as follows:

1. One of the theory is that there was water scarcity in the city due to drying of lake or maybe the water was not enough for the rising population. But this is quite hard to believe as there was a very advanced and detailed water supply system. Moreover the travellers also mentioned that the lake was very large.

But still this is one of the most accepted theory all over

2. Another reason because of which Akbar chose to stay in Agra may have been that Fatehpur Sikri was not a citadel. It was placed as an open and courtly city which was hard to defend (Gupta, 2013).

Derivations from Fatehpur Sikri

1. This city of Fatehpur Sikri has no streets but consists of a series of interlocking courtyards set to the cardinal points. The individual monuments are designed in symmetry but in the overall planning of complex asymmetry is used. The planning was very open and welcoming which is missing in today's cities.
2. Moreover it also teaches us how a small negligence on planners part can ruin the future of whole city and lead to wastage of our resources. The same this happened to Fatehpur Sikri due to water scarcity
3. Akbar's this city welcomed everyone without considering their religion. In the same way todays city should be designed so that the people of all religions can live their together.

References

1. Ali A. Syncretic architecture of Fatehpur Sikri: A Symbol of Composite Culture. Journal of Islamic Architecture, 2014.
2. Dix AP. Fathepur Sikri. Germany: Antiquariat Willi Braunert, 1993.
3. Gupta SS. Fatehpur Sikri: Akbar's Magnificent City on a Hill. New Delhi: Niyogi Books, 2013.
4. Koch E. Mughal Architecture: An Outline of its History and Development, Primus Books, 2013, 1526-1858.
5. Nath R. Fatehpur Sikri and Its Monuments. Historical Research Docu. Pro. Peck, L. (2014). Fatehpur Sikri. Lustre, 2000.
6. Sharma DP. Indo-Islamic Architecture (Delhi and Agra). Winsome Books, 2008.
7. Shaukat Mahmood ZD. Revisiting the Legacy of Fatehpur Sikri. Malaysia: Lium Press, 2017.
8. Singh S. The Architecture of Fatehpur Sikri. Aligarh: Aligarh Muslim University, 1995.

Chapter - 4
Analysis Big Data and Machine Learning based Sustainable Smart Cities in India

Authors

Konala. Uma Devi
Assistant Professor, Department of CSE, BVC College of Engineering, Amalapuram, Andhra Pradesh, India

G.V.V. Sita Maha Lakshmi
Assistant Professor, Department of CSE-IoT Malla Reddy Engineering College, Hyderabad, Telangana, India

Chapter - 4

Analysis Big Data and Machine Learning based Sustainable Smart Cities in India

Konala Uma Devi and G.V.V. Sita Maha Lakshmi

Abstract

A Bigdata is the vast information storage collected from various locations and sources. Bigdata is defined as centralized repository with a standard structural specification. But the information driven from various sources are not always appropriate for this structure. Recent technological advancements in typical domains (e.g. internet, financial companies, health care, user generated data, supply chain systems etc.) have directed to inundate of data from these domains. Because of the huge reduce in the overall investment and greatest flexibility provided by the cloud, all the companies are nowadays migrating their applications towards cloud environment. Cloud provides the larger volume of space for the storage and different set of services for all kind of applications to the cloud users without any delay and not required any major changes at the client level. When the large amount of user data and application results stored on the cloud environment will automatically make the data analysis and prediction process became very difficult on the different clusters of cloud. Whenever the used required to analysis the stored data as well as frequently used services by other cloud customers for the same set of query on the cloud environment hard to process.

Keywords: Machine learning, bigdata analytics, smart cities

1. Introduction

Big data is considered as the vast collection of datasets obtained from various sources. This data organization architecture suffers from various complexities in terms of larger dataset, complex query handling, security, distributed shared environment, visualization features etc. To handle this, there is the requirement of management tools so that effective information extraction and query processing will be done. Each data representation task in big data is represented by a separate tool. The foremost operation on big

data environment is data acquisition. The data is here taken from various sources distributed at different location. The complexity in data acquisition process is the structural difference in the datasets taken from various sources. This difference can be identified in terms of number of attributes, type of attributes etc. Big Data, Cloud computing are the buzz words for the future of IT industries. As per the latest survey by IDC [1-2] it has been seen that social sites are creating a huge amount of data per day like from twitter site almost 700 million tweets are sent, From Youtube 5 million hours of content is uploaded, 6 billion searches are done on Google, 4.2 billion of likes comes from Instagram, whereas 5.75 billion of likes done on Facebook, 5.1 billion of messages by Facebook [3-4]. Big Data is derivative of the trend that followed Data Explosion. Data is the only thing constantly increasing and transforming our society. Bigdata is very diverse in nature. Fundamentally, Bigdata characterize as not only a huge volume of data it basically consist of set of unstructured, semi-structured and structured which cannot be stored in simple table formats. There are many definitions available for big data here in this paper we summarize definitions from attribute, comparative and architectural point of view, which play an important role in modelling how one can view big data. Below we defined definitions of Big Data from these three aspects [5]:

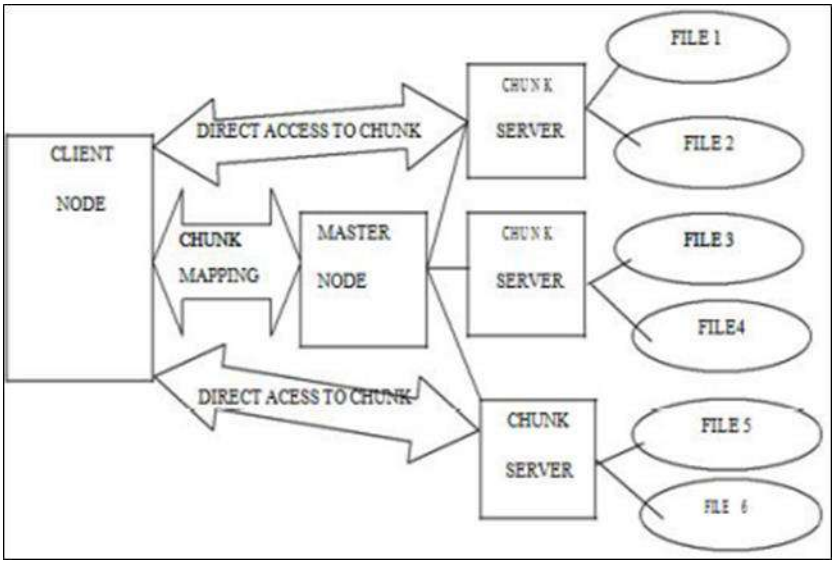

Fig 1: Bigdata Data Process

2. Big Data Analysis

A) Business Data

The typical data collected for big data processing is from different organization or the companies such as RFID data, CRM data systems, ERP data sources and web store transactions.

B) Machine Generated Dataset

There are number of automated machine based system that capture the data itself using smart devices or the sensors and upload in the datastores. Auto call detail, smart meter processing, weblog processing, equipment data processing, automated trading systems, traffic sensor analysis etc.

C) Social data

This kind of data is obtained by different web sites by taking the user comments or feedback. Different blogging and social networking sites are associated with it. This kind of data includes different language form that requires intelligent conversion of language in normal form. Once the data is collected, the next work is to manage the on bigdata servers. There are number of available server tools to manage such dataset.

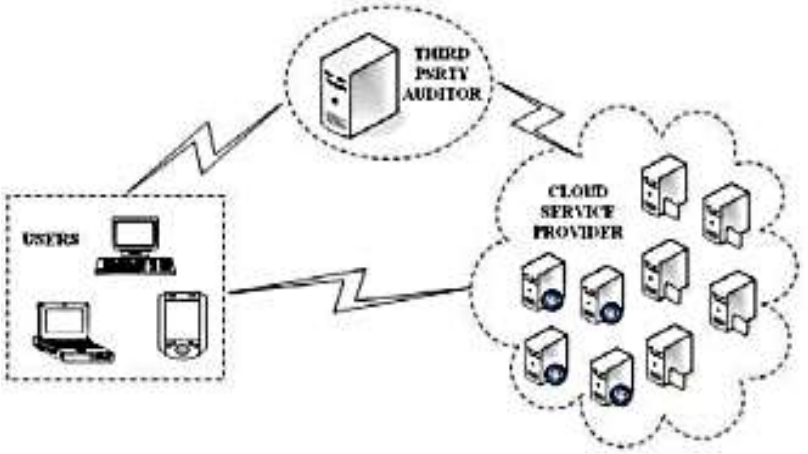

Fig 2: Representative traditional architecture

User data stored on the cloud environment divided in to number of chunks. Each chunks will be stored in the different cluster of different server on the cloud environment. Unique id will be provided for the data for the identity of the user. Based on the unique id the data can be distributed and maintained geographically in the different servers in different locations.

Cloud storage is built on the network computing environment. There are many benefits to move data into the cloud [6-7]. For example, users do not have to care about the complexities of direct hardware management. But since users store their data in the cloud, it means that they will lose the control of them and more and more worries will come out about the data security The data stored on the cloud storage as a service trend analysis is the major work for the customer as well as the cloud service provider to identify the interest of the user from the database.

D) Data Acquisition

Data acquisition phase is divided into data collection where data is obtained from various data sources, Data transmission phase and then data pre-processing phase from which useful information is obtained.

E) Data Storage

The data storage is always required to keep the data needed for future use hence a data subsystem in a big data platform organizes the collected information in a format which can be used for the exploration and value abstraction purpose. The data storage consist of the two parts mainly: Hardware arrangement and for managing data: data management system is required.

F) Data Analysis

Analytical methods or tools are required to inspect, transform, and model data to extract meaningful value. It has certain purposes like to understand the meaningful information from the data and what value added functions can be added to the given data.

G) Data Generation

Data generation is the first main phase of Bigdata. Data sources such as sensors, social sites, health care centers, satellite, air plane, media, business apps, machine log data, generate large, diverse, and complex datasets. Figure1 depicts data generation phase which shows that the data source attribute values are mainly from the scientific field, business field and the networking field. Scientific field produce very low whereas business field produces very high attribute value and the networking field produces very high data rate**.**

3. Machine Learning Approach

Dataset: Dataset is the actual structured information set obtained from various sources. Each dataset is here described with relative metadata

information. This metadata will explain the dataset constraints and priorities. If some transformation is required that will also be represented in the dataset. In this work, a bigdata acquisition is performed from m different datastes called D1,D2….Dm

Transaction: A transaction is considered as the entry made to any of m dataset from any dataset user. A transaction will be considered valid if user has input the minimum data requirements in specified dataset. Each dataset is having n number of transactions in it. A data set is considered as the group of n transactions

SUP: It is considered as the transaction measure under the associativity. The association support between two transactions represented by SUP(A->B). It actually represents the number of transacton that are contains both A and B. Here support is the machine vector that generates a rule to identify the valid value required for acceptability. If the outcome is lesser than SUP value, it can be discarded. Such value that defines the lower limit is called MinSUP.

CONF: It is considered as the certainity analysis rule defined under associativity analysis. The Conf Rule is defined by CONF(A->B) and represents the number of transaction that are having both A and B / Transaction in A. The conf value actually represents the strengthen vector a specific value under transaction analysis. MinCONF is represented as the vector that represents the strengthen associated in transaction.

ASSO: It is considered as the associativity rule defined under machine learning applied on transactions under the SUP and CONF vectors. The associate activity represents the relationship between to items or data values called A and B. This rule representation is defined as A -> B where A ∩ B =null. Once these all terms are defined, the next work is to apply the machine learning theorm over it to increase the dataset reliability. To obtain the certainity and the effective outcome, the measurement is here performed under MinSUP and MinCONF vectors. The process stages or the algorithmic specification of this machine learning rule set is given here under Let's consider the following infrastructure facilities inside a smart home. Imagine coming back home in the evening and our house wakes up. This is not a dream of the future, thanks to the boom in sensor technology. Smart Homes, also known as automated homes, intelligent buildings, integrated home systems or domestics, are a recent design development [8].

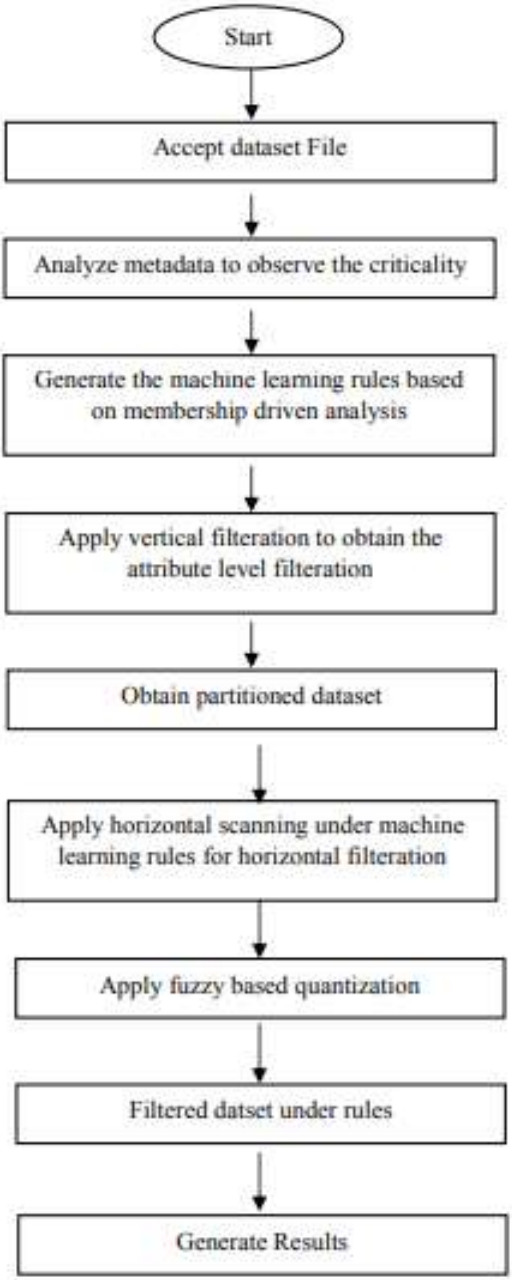

Fig 3: Flow chart of Machine Learning Approach

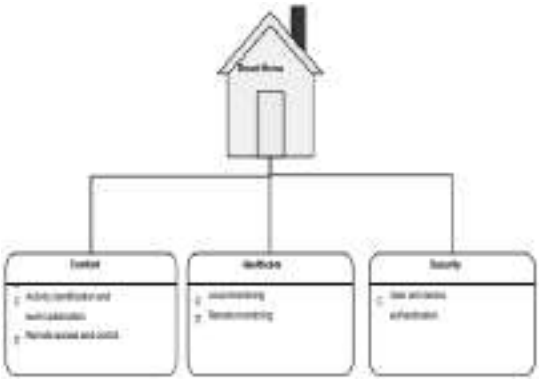

Fig 4: Desired for decipherment

An indistinguishable key is desired for decipherment as well as decipherment. On the contrary in asymmetric key encoding, pair of keys, that is to say a public key and a private key, are utilized for data decipherment as well as decipherment. So, peers of both the keys are significant in all cryptographic system. The fundamental objective of cryptography is to enable the transmission of message from the source to its equivalent destination via a transmission channel in a manner so that the message all through its transmission cannot be intercepted by someone.

Through the networking of individual system modules, preset scenes can be executed to make your everyday life safe and comfortable. Imagine when you reach your house the garage door opens, drive way is sufficiently illuminated, blinds are raised and alarm system is deactivated and when you leave your house also this technology puts your house to the rest at the touch of a button you can be sure that your lights are switched off, the blinds are lowered lobbies are at rest and heating is turned down and the alarm system is activated. The door communication station installed at the entrance is extremely robust, it is weather resistant and housing solid metal buttons as well as the single paint illuminated glass nameplates. The station can only be dismantled using a special tool, its well protected against the sabotage, depending on the system configuration when the bell button is pressed in the dark, the exterior lighting is switched on to welcome your visitors. Optimum communication and safety is of course always guaranteed. The camera which is not visible externally supplies sharp images and the digital signal processor guarantees the best speech quality. The image which is transmitted externally is transferred onto high quality TFT color monitor of the indoor station. It’s possible to shift or zoom in on the image detail via the onscreen display with touch function. The proposed system does not require a

dedicated server PC with respect to similar systems and offers a novel communication protocol to monitor and control the home environment with more than just the switching functionality [9-10]. For the best communication condition the integrated full duplex operation with the digital signal processor enables error free and synchronous speech as well as making a telephone call moreover the automatic calibration to the ambient conditions and active suppression of street noise optimizes the comprehensibility. The indoor station has audio and video function, a simple and convenient adjustment and operation is guaranteed by the touchscreen and large push button. Individual messages are recorded and saved with the voice memo function, if a message has been left, an LED on the keypad flashes by wave indication, the message can still be received. When the door bell is pressed the camera image is automatically stored together with the time of date. It can be determined at any time who was at the door while you are away. The menu is retrieved by touching the info I button on a menu on the machine inside your door, after selecting a memo and image the chronologically stored messages are clearly displayed, you can then select or simply retrieve the picture message using the arrow keys. You will be greeted in the house thanks to the communicating IoT technology. The internal blinds are raised and ceiling lights are switched on, other such scenes can also be programmed using a give controller. With the presence detector you can control the lighting in the room using a presence detector, this saves energy as the light only switched on without fail when someone is actually in the room. The LED pilot lights with the download outlet will illuminate the stairs so that they can be seen at any time and creates optimum safety at the stairs even when the ceiling lights are switched off. The right mood is always created with the room controller even in the quite room weather it's a game of chess or a cozy evening by the fire just click on the buttons on the room controllers. Thanks to the LED outlets you can avoid switching on the lightings when walking through the room in the dark. The integrated pilot light is sufficient and makes you way trip hazards in good time. The kitchen diner as the focal point of the house is ideally suited for the IoT home controller. It's clearly understandable touch screen enables functions throughout the house to be managed.

4. Enabling IoT and Big data

The central functions of your house can be controlled and visualize without any problem via the control panels installed individually in the room. With the intelligent facility pilot software, for example a bundle of windows application standard interface, this type of control is also possible

via any PC. The facility pilot creates the link for the implementation of multi-rooming you can therefore listen to the news in the kitchen, rock music in the bathroom and a radio play in the children bedroom. Smart metering provides all the intelligent and efficient handling of the energy is the current topic. It would seem logical to continually record, display and evaluate the consumption values for the electricity, water and thermo-energy with the facility pilot. This facility pilot informs you at a glance about the security status of your house, you can see whether any and if so which doors and windows have been opened, existing network cameras are visualized here and you can see what's going on, in or near the house. The more expensive our primary energy becomes the more innovated and sophisticated heating control system is, this task is made easier with the facility pilot who likes going from room to room adjusting the thermal stat depending on demand and presence. Thanks to the visualization screen you can see set points and actual temperatures in all the rooms at a glance and influence them. Blinds, shutters and curtains also contribute to heat protection, against solar radiation in the summer and reduction in heat transmission in the winter. Automatic time and weather dependent control is absolutely recommended. The lighting control via the facility pilot has two benefits, increased convenience and energy savings. In addition to the possibility of switching and dimming the lighting from one location the software can of course do much more for example combined several light fittings and blinds in one area into individual scenarios. A room combo sensor on the roof supplies the weather data in connection with the weather station. The connection is carried out by the facility pilot. The facility pilot can even display the internet content via its browser function as soon as its linked to a network with internet access via its LAN interface whether its simple surfing or the complete remote interrogation of your building functions, the facility pilot offers you the full range. The energy saving automatic switch ensures that the light is switched on as soon as someone is located This grass will also filter the treated water which can again be used anywhere else in the city because there is a lot of nutrient uptake which will be given by the grass and consumed by the grass, thus we can make a beautiful landscape out of it. We will also plant some special kind of trees in our smart city, we don't just want beautiful trees, the landscape or shrub we also want to have trees that are going to bring something back to us, so for example the date palm needs to be pollinate in the spring and then we're going to harvest the dates in August and then the trees which will be scattered along the farm, we will have avocado, papaya, pomegranates, mulberry, fig trees so those are spreads and they will benefit from the shade of the palm trees and all of that is actually

irrigated and treated. The running along pipes across the city will be installed everywhere and they will actually carry treated sewage actually which will be used to water those plants.

5. Results and discussion

The pruning over the dataset is performed in under different impurities cases. These cases includes the missing value analysis, lack of associativity analysis etc. The filteration of records over the dataset is shown in table. The table is showing the valid rules obtained from the dataset. The values that satisfy these rules are considered as valid dataset instances**.**

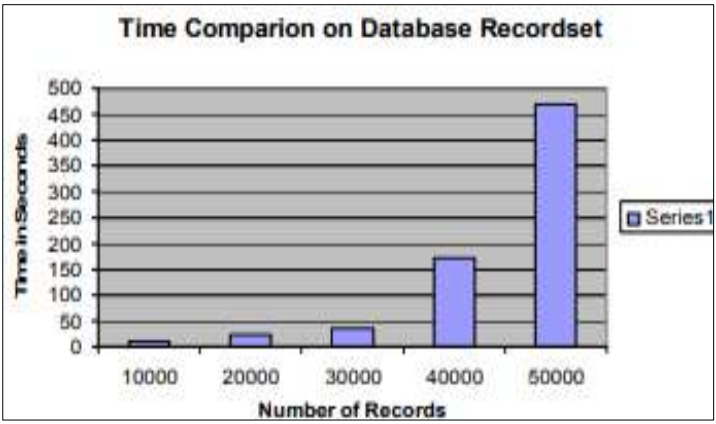

Fig 5: Dataset filtration

The figure shows the effective exploration of rules based on which the dataset filtration can be done effectively. The presented machine learning approach has identified the valid rule set based on which the dataset records can be validated.

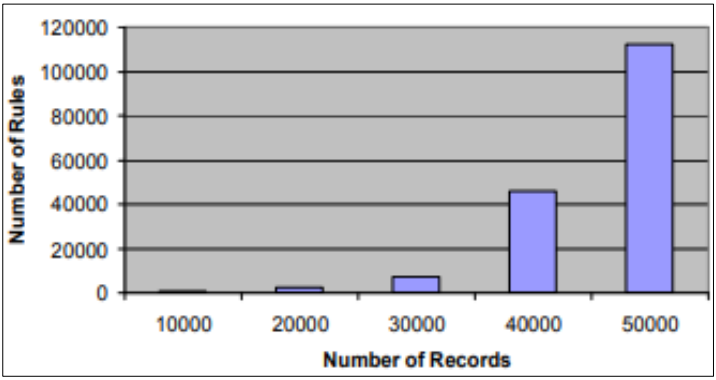

Fig 6: Dataset filtration

Let us consider, most of the cloud users interested for server machine software windows server 2008. Then the cloud service provider can offer the winserver 2008 for the same set of user request from the client. Using frequent data item set identified through bigdata map reduce function, cloud server analyze the entire cloud database for the same set of services and recommend to the user for most user frequent service can rapidly increase the number of users in the cloud environment.

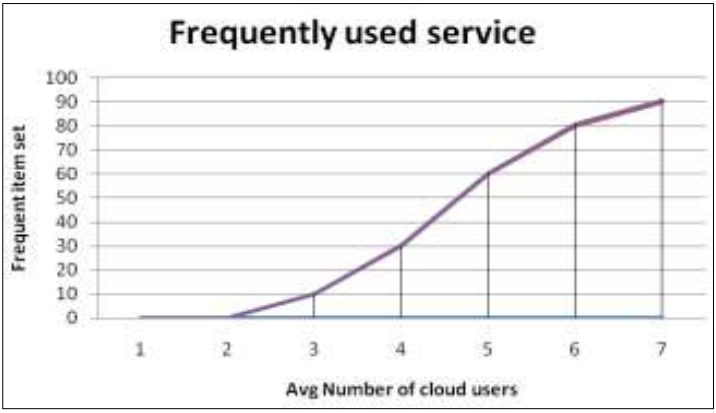

Fig 6: Dataset filtration curve

The interoperation between the cloud storage servers and the trustful organization's servers in scheme are designed as follows. Description of exchanging process it is worth nothing that all these process are done by the authentication modules in the cloud storage servers and it does not have any relationship with other modules.

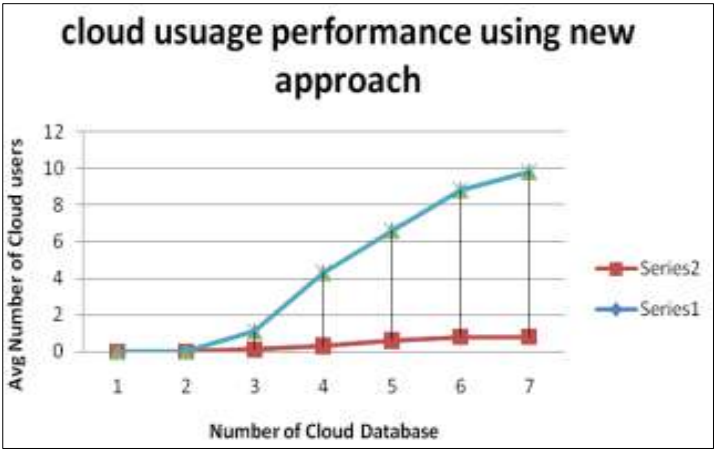

Fig 7: Dataset filtration curve

Table 1: Data set values

S.No.	PROPERTIES	NoSQL	NewSQL	Map Reduce	HIVE	HBase
1.	Scalability and High performance (Horizontal/Vertical)	Yes (Horizontal)	Yes (more preferred)	yes	Yes	Yes
2.	Flexibility (data formatting)	Yes	Maybe	Yes	Yes	No
3.	Ability to run on different commodity hardware	High	High	High	High	Less
4.	Security	Less	Less	More Secure	More	More
5.	Partition Tolerance	Yes	Maybe	yes	Easy to partition data	Difficult to partition
6.	Consistency and integrity	Not useful	Useful	Not useful	yes	Not useful
7.	OLAP	Yes	Yes	Yes	Yes	Yes
	OLTP(Real time read/write)	No	Yes	No	No	Yes
8.	ACID Property	No	Yes	No	Yes	No
9.	Costs of commodity hardware	high	Low	Low	Low	Low
10.	SQL Interface	No	No	No	Yes	No
11.	Schema used	Schema Free	Schema needed	No schema	Schema needed	Schema free
12.	Usage	Easy	Easy	Less difficult	Easy to use	Difficult to use

Conclusion and future scope

Conclusion

This work aims to provide an optimized data analysis technique for the cloud storage from multiple cloud clusters. Also proposed scheme trying to analyze the trend by identifying frequent service used by the other users using Map-reduce algorithm. By utilizing the new scheme will increase the number of cloud users on cloud environment also reduce the complexity to find frequent services in cloud computing, In the proposed scheme using Map-Reduce algorithm and Big Data analysis techniques achieves the better performance compared to the existing techniques. In this paper, the concept of Bigdata and the Bigdata value chain has been highlighted which covers the entire big data lifecycle. A simple definition for Bigdata used here is, it is a large amount of unstructured data produced.

References

1. Yan Chen, Wang Peng, Pang Haitian, Sun Lifeng, Yang Shiqiang. CELoF: Wi-Fi Dwell Time Estimation in Free Environment. 2017;10132:503-514. 10.1007/978-3-319-51811-4_41.
2. Singh Isha, Sigg Stephan. Smart City Environmental Perception from Ambient Cellular Signals, 2017, 695-704. 10.1007/978-3-319-65482-9_55.

3. Angelova Liliya, Flikweert Puck, Karydakis PanagIoTis, Kersbergen Daniël, Teeuwen Roos, Valečkaitė, Kotryna *et al*. 148 DynamIoT - Geomatics Synthesis Project on IoT, 2017. 10.13140/RG.2.2.22116.27528.

4. Griego Danielle M, Buff Varin, Hayoz Eric, Moise Izabela, Pournaras Evangelos. Sensing and Mining Urban Qualities in Smart Cities, 2017. 10.1109/AINA.2017.14.

5. Fernández Ares Antonio, Mora Antonio, Arenas MG, GarcíaSánchez Pablo, Romero G, Rivas Santos *et al*. Studying real traffic and mobility scenarios for a Smart City using a new monitoring and tracking system. Future Generation Computer Systems, 2016. 76. 10.1016/j.future.2016.11.021.

6. Nazari Mohamad Esmaeil. Smart Grid Unit Commitment with Considerations for Pumped Storage Units Using a Heuristic Optimization Algorithm, 2018.

7. Bracco Stefano, Delfino Federico, Ferro Giulio, Pagnini Luisa, Robba Michela, Rossi Mansueto *et al*. Energy planning of sustainable districts: Towards the exploitation of small size intermittent renewables in urban areas. Applied Energy. 2018;228:2288- 2297. 10.1016/j.apenergy.2018.07.074.

8. Strasser Thomas, Siano, Pierluigi, Ding Yi. Methods and Systems for a Smart Energy City. IEEE Transactions on Industrial Electronics. 2018;66:1363-1367. 10.1109/TIE.2018.2869488.

9. Dominković Dominik. Modelling Energy Supply of Future Smart Cities, 2018. 10.11581/dtu:00000038. 149

10. Guan Zhitao, Si Guanlin, Zhang Xiaosong, Wu Longfei, Guizani Nadra, Du Xiaojiang *et al*. Privacy-preserving and Efficient Aggregation based on Blockchain for Power Grid Communications in Smart Communities, 2018.

Chapter - 5
Fake Audio Detection using Machine Learning Techniques

Authors

Anurag Bhatnagar
Department of Information Technology, Manipal University Jaipur, Dahmi Kalan, Rajasthan, India

Yamini Agiwal
Department of Information Technology, Manipal University Jaipur, Dahmi Kalan, Rajasthan, India

Chakravardhan Rao
Department of Information Technology, Manipal University Jaipur, Dahmi Kalan, Rajasthan, India

Chapter - 5

Fake Audio Detection using Machine Learning Techniques

Anurag Bhatnagar, Yamini Agiwal and Chakravardhan Rao

Abstract

Deep neural network model advancements have led to notable improvements in false sound creation. Therefore, it becomes more crucial than ever to create foolproof yet lightweight systems for false sound detection. Training with graphics, videos, and audio has gotten easier and more user-friendly. We still must deal with some dangers and drawbacks. In this post, we'll talk about the frightening sound produced by deep fakes, a term that's very common in cutting-edge technology. The use of false sound can be detrimental and have an impact on human existence either directly or indirectly. For instance, deep learning navigation is used by Google Maps; if changed, we will be redirected. There were numerous papers on how to differentiate real or false sound. To accomplish the task, Python and deep learning were employed. The input for this work is audio or video data, and the model was trained for specifically recognizable features for voice production and voice identification. The accuracy between real and fake is determined using the deep learning technique.

Keywords: Fake audio, spoof, python, machine learning

I. Introduction

Recent advances in deep learning have led to dramatic improvements in the automatic generation of natural-sounding audios. This has led to their use in a wide variety of applications, including the design of assistive technology, educational technology, and games. Unfortunately, they can also be used as a powerful tool to spread false information and to thwart automatic speaker verification and voice biometrics systems. For example, audio deepfakes spreading false political narratives were seen as a significant threat to the 2020 United States presidential election. Audio deepfakes have also been successfully used to trick ASV systems, where in one case, they allegedly resulted in a loss of USD 243,000 via a fraudulent bank transfer. These examples highlight the extent of the potential damage from natural-

sounding tampered audio as well as the vulnerability presented by the ASV system. To automatically distinguish between synthetically and bona fide generated audios, several data- and knowledge-based countermeasure models have been proposed. While deep learning-based models achieve high performance by automatically extracting discriminating features from audio files, they require a large amount of training data and computational resources. ASV Proof Challenge can help provide different language with different tone of voice and the second thing is any technique of deep learning and python computing function to differentiate real or fake audio speech. There are two types of ASV dataset; text-dependent and text-independent. Language tone and content with audio features are required depending on the text; it uses i-vector probabilistic linear discriminant analysis Utilizing Mel Frequency coefficients, independent text works with several languages to extract features from audio. We demonstrate 80-85% accuracy in detecting a real or false audio sample utilising a susceptible system. ASV datasets come in two varieties: text-dependent and text-independent. Depending on the text, language tone and content with audio features are needed; i-vector probabilistic linear discriminant analysis is used. Utilizing Mel Frequency coefficients, independent text works with several languages to extract features from audio. We obtain 80-85% accuracy in detecting a real or false audio clip utilizing a. ASV datasets come in two varieties: text-dependent and text-independent. Depending on the text, language tone and content with audio features are needed; i-vector probabilistic linear discriminant analysis is used. Utilizing Mel Frequency coefficients, independent text works with several languages to extract features from audio. We demonstrate 80-85% accuracy in detecting a real or false audio sample utilizing a susceptible system. Utilizing Mel Frequency coefficients, independent text works with several languages to extract features from audio. We demonstrate 80-85% accuracy in detecting a real or false audio sample utilizing a susceptible system. Utilizing Mel Frequency coefficients, independent text works with several languages to extract features from audio. We can obtain 80-85% accuracy when determining whether an audio sample is authentic or phoney using a susceptible system.

I. Deep fake audio generation

It is possible to extract the language into a Meta representation with the aid of divine deep learning and then synthesize the sound using this representation. When trained on 30 or more recordings, the online platform provided by Montreal-based AI startup Lyrebird can mimic a person's voice. The voice of a person may be synthesized by Baidu using just a few audio

samples thanks to a new neural voice cloning method it unveiled last year. A text-to-speech synthesis system typically consists of many steps, including an audio model, an audio synthesis module, and a user interface for text analysis. On the ideal neural network architecture for TTS, there is currently no agreement. The end-to-end synthetic text-to-speech model creates speech from the characters themselves. Format for single-speaker TTS systems. Pair for multi-speaker TTS systems. The text preprocessing was performed in uppercase all characters in the input text. The pause interval can be estimated using a text-audio format tool such as Soft Voice Conversation which is the process of converting the source speaker's voice into a sound like that of a voice of the target speaker. The VC processes information related to segmentation and hyper segmentation features and keeps the linguistic content similar. Embed Adaptation and voice conversion. Adaptive, a model is already independent, and it gives visible B-wave output.

A multi-speaker synthesis model will consider English phonemes that were trained to anticipate new speaker embedding. The target speaker's speech is synthesized using Net2. A series of utterances made by the target speaker constitute the input/target. The public dataset will be the target1arctic dataset, while the private dataset, target2, will contain more than 2 hours of sentences from the audiobooks she reads. In this case, the goal is to accurately reproduce a new speaker's voice in a matter of minutes or even seconds using a synthetic model that can be trained from scratch using a huge number of audio samples. This presents a problem because the model must generalize to invisible texts while learning the features of the speaker from a very small amount of input. Learning based on Text-to-Speech synthesis models, such as the Audio model, learns to generate the character text of the spectrometer form, and the encoder model learns to generate the sound wave from the spectrometer. For the speaker to adapt to part of the model, selected classes of the pre-trained TTS model were trained with PT data. We need some basic ingredients such as Attention-based sequential models are widely used in machine translation, speech recognition and text summarization. In speech synthesis, synthetic models can be tailored based on the text and the identity of the speaker. While the text carries linguistic information and controls the content of the speech produced, speaker identity captures characteristics such as pitch, rate of speech, and stress. The neural encoder takes the lost spectral maps and overlays the natural layer. Technically, the neural encoder is responsible for inverting these spectrograms back to audio in phase reconstruction. Libri voice requirements 24 hours and more speakers. A generative model with numerous speakers will be used to apply English phonemes that have been

taught to anticipate the addition of additional speakers. The speeches of the target speaker are synthesized using Net2. The target speaker's series of statements serve as the input and destination. The Arctic dataset will be the target1 of the datasets, which are open to the public, and the other datasets will be the target2 of more than 2 hours of privately read audiobook phrases. In this case, we concentrate on cloning the voice of a new speaker using a few minutes or even a few seconds of data. The generative model can be trained from scratch with a vast number of sound samples. This is difficult since the model needs to learn the speaker's features from a relatively small and very limited amount of data and still generalize to invisible texts. Learning-based text-to-speech synthesis models, e.g. the vocoder model learns to generate a sound wave from the provided spectrograph, and the acoustic model learns to generate a spectrograph from the character text. Selected layers of the pre-trained TTS model were trained using PT data in order to adapt the speakers to a particular component of the model.

We need some fundamental elements, such the fields of machine translation, speech recognition, and text summarization all make extensive use of attention-based sequence models. Generic models for speech synthesis can depend on the speaker and text's identities. The identity of the speaker captures details like pitch, rate of speech, and accent while the text conveys linguistic information and determines the substance of the generated speech. A feature of the neural vocoder is the ability to capture lossy spectrograms. Overlaying another layer of naturalness. A neural vocoder's role, technically speaking, is to convert these spectrograms back to audio while reconstructing the phase.

24 hours and multi-speaker Libri speech requires

A single-speaker model may require ∼20 hours of training data, while a multi-speaker model for 108 speakers requires approximately 20 minutes of data per speaker.

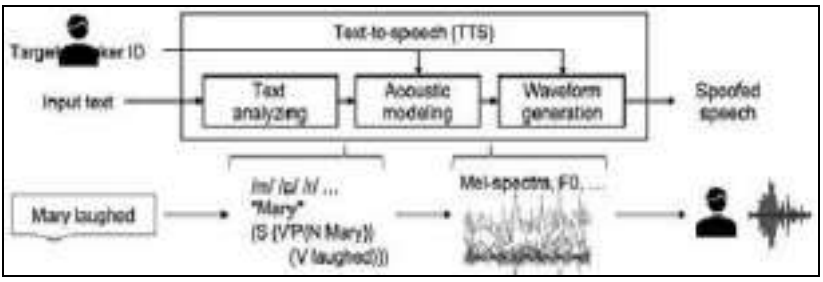

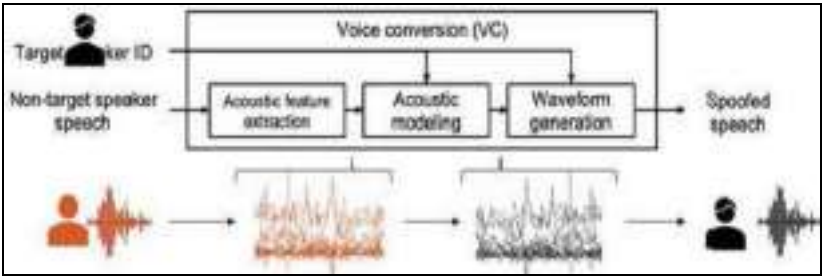

Deep fake voice detector

In general, the terms "speaker identification" and "speaker verification" are used interchangeably. The speaker verification system automatically determines whether the identity declaration is genuine or false while the speaker identification system recognizes who the speaker is. The ASV system is susceptible to spoofing attacks like as impersonation, replaying, twinning, and speech synthesis.

A generic ASV system is strong and simple to tamper with; they are more susceptible to complex attacks. Such a weakness is one of the security issues with ASV systems. To access the system, the adversary engages in phishing by pretending to be the target speaker. Different biometric features, such as fingerprints, irises, faces, and speech patterns, can be the target of such spoofing attacks. For the ASV, we only concentrate on voice-based anti-spoofing and anti-spoofing strategies. Google's ASV 2019 spoof dataset contains more than 25,000 audio clips, including real and fake clips of various male and female speakers. The model receives its input from the preprocessed, primary frequency histogram created from the raw audio. To avoid overfitting, the model runs the spectrogram in time-dimension iterations before using masked compositing. After passing the output through a dense layer and a sigmoid activation function, a prediction probability between 0 and 1 is finally produced. The underlying model achieves 85% on board, validated, and tested, 99% and 95% accuracy, respectively. The disparity in performance between the three datasets is the cause.

Conceptual overview

CNN is one of the most popular types of neural networks used for image recognition and classification. CNN is commonly used in fields like object detection, face recognition, etc. Image classification CNN takes an input image, processes it and classifies it into several groups. The input image is viewed by the computer as an array of pixels with a variable number of pixels depending on the resolution of the image. The code for the Convolution neural network is written in Python using the Keras package.

Nuclear operations in the convolutional layer from the time domain, the audio splits are transferred to the frequency domain. The result of this process is an amplitude spectrum. The MFCC function is one of the most important methods of extracting a function from an audio signal and is commonly used when working with audio signals. The mel-frequency cepstral signal coefficient is a short group of properties that briefly define the overall shape of the spectrum envelope.

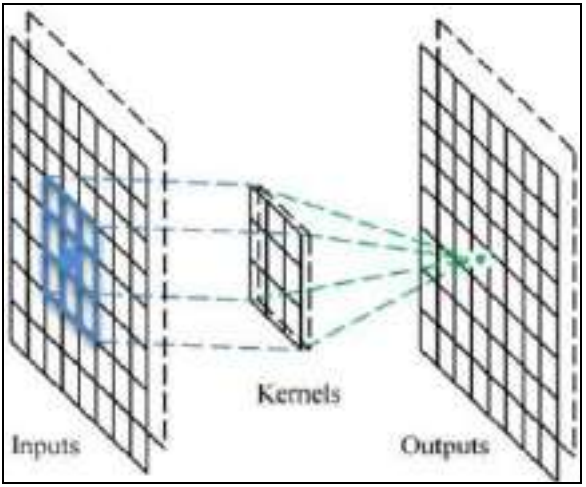

II. Technologies involved

Google Colab: Colaboratory or "Colab" for brief, is a product from Google analysis. Colab permits anybody to jot down and execute whimsical python code through the browser, and is very likeminded machining learning, knowledge analysis and education. Google Colab is employed as associate atmosphere thanks to the free availableness of GPU to accelerate model performance.

Librosa: Librosa is a sturdy Python package for operating with and analyzing audio. it is the opening move toward addressing audio knowledge at scale for a spread of applications, from distinctive a human voice to extracting personal options from audio and free underneath the Apache two.0 ASCII text file license. The API is nominally for the Python artificial language, though there's access to the underlying C++ API.

Conclusion

ASVspoof has addressed two different spoofing scenarios, Logical Access, and Physical Access, as well as three main forms of spoofing attack: synthetic, transformed, and replayed speech. The LA scenario aimed to

determine whether advances in countermeasure design kept pace with progress in TTS and VC technologies and, as a result, whether today's cutting-edge systems pose a threat to the reliability of ASV. While the findings show that the newest techniques, such as those using neural waveform models and waveform filtering, in addition to those resulting from transfer learning, do indeed cause greater degradations in ASV performance, there is potential for their detection using countermeasures combining multiple classifiers. PA scenario, aimed to evaluate the leak threat and countermeasure performance through simulation, where factors influencing replay fraud attacks can be carefully controlled and studied. The simulations consider changes in room size and reverberation time, playback device quality, and physical separation between both speakers and attackers and between speakers and the ASV system microphone. Regardless of the replay configuration, all replay attacks degrade ASV performance, but reassuringly, there is promising potential for this. It considers changes in room size and reverberation time, playback device quality and physical separation between both speakers and attackers.

References

1. "Asvspoof: the automatic speaker verification spoofing and countermeasures challenge evaluation plan, 2019. http://www.asvspoof.org/asvspoof2019/asvspoof2019evaluation plan.pdf, 2019, [Online].
2. ASVspoof: Automatic Speaker Verification Spoofing and Countermeasures Challenge Evaluation Plan∗ Tomi Kinnunen1, Nicholas Evans2, Junichi Yamagishi3, Kong Aik Lee4, Md Sahidullah1, Massimiliano Todisco2, H´ector Delgado2, 2017.
3. ASVspoof: The First Automatic Speaker Verification Spoofing and Countermeasures Challenge Zhizheng Wu1 Tomi Kinnunen2 Nicholas Evans3 Junichi Yamagishi1 Cemal Hanilc¸i2 Md Sahidullah, Aleksandr Sizov, 2015.
4. Fake Audio Speech Detection: Shilpa Lunagaria1, Mr. Chandresh Parekh2 1 Student at M. Tech, School of Information Technology & Cyber Security, 2Dean, School of Information Technology & Cyber Security, Raksha Shakti University, Lavad, Dahegam, Gandhinagar, Gujarat, India
5. Fake Audio Detection in Resource-constrained Settings using Microfeatures Hira Dhamyal, Ayesha Ali, Ihsan Ayyub Qazi, Agha Ali Raza Lahore University of Management Sciences, Pakistan.

6. Computer Science Wiki, “Max-pooling/Pooling”, 2018. https://computersciencewiki.org/index.php/Max-pooling_/_Pooling, (Mar. 1 2021)
7. Mahajan P. “Max Pooling”, 2020. https://poojamahajan5131.medium.com/max-pooling-210fc94c4f11
8. McFee Brian, Colin Raffel, Dawen Liang, Daniel PW Ellis, Matt McVicar, Eric Battenberg, *et al*. librosa: Audio and music signal analysis in python. In Proceedings of the 14th python in science conference, 2015, 18-25.
9. Chollet F. Keras. GitHub, 2015. Retrieved from https://github.com/fchollet/keras

Chapter - 6
Classification of Covid-19 and Pneumonia chest X-Ray and CT images using Various CNN Models

Authors

Anurag Bhatnagar
Department of Information Technology, Manipal University Jaipur, Jaipur, Rajasthan, India

Vibhor Sharma
Department of Information Technology, Manipal University Jaipur, Jaipur, Rajasthan, India

Chapter - 6

Classification of Covid-19 and Pneumonia chest X-Ray and CT images using Various CNN Models

Anurag Bhatnagar and Vibhor Sharma

Abstract

Millions of people have been affected with the coronavirus illness 2019 (COVID-2019), which first surfaced in Wuhan, China in 2019 and has rapidly spread over the world since the start of 2020. The fight against the COVID-19 pandemic has emerged as one of the most promising issues in global healthcare. To receive the best medical care and stop the pandemic, COVID-19 cases must be precisely and speedily detected. After that, the virus spread throughout the entire planet, with over 4.7 million verified cases and more than 315000 fatalities as of the time this report was being written. As a decision support tool, radiologists can use machine learning algorithms created on radiography images to help them complete diagnoses more quickly. Several papers have been published to help with detection and reduce the spread of the virus.

This project has reviewed several research papers on the topic of Covid-19 detection and discusses various methods and techniques used by researchers to identify the virus using chest X-Rays and CT images.

Keywords: COVID-19, pneumonia chest X-Ray, CT images, radiography

Introduction

Since initially appearing in Wuhan, China, December 2019, the severe acute lung syndrome-causing coronavirus 2 (SARS-CoV-2) began to spread internationally. The infection's mortality toll is rising at an alarming rate, and many health systems throughout the world are trying to keep up. In order to stop the spread of this viral infection, the World Health Organization (WHO) has recommended a range of tactics, including social isolation. Effective and accurate COVID-19 patient screening is a critical step in this strategy so that those who test positive are treated right away and appropriately isolated from the general population. The severity of the illness is more closely linked to old age. In cases of severe illness, pneumonia is the most prevalent complication.

Patients with pneumonia frequently experience symptoms like fever, exhaustion, a dry cough, anorexia, myalgia, dyspnea, and the production of sputum. The use of radiological imaging in the diagnosis of lung disorders is crucial. CT scans demonstrated ground glass opacification in COVID-19 infection, which was frequently bilateral and included the peripheral area of the lower lobe of the lungs, and the radiological abnormalities might be present even in preclinical instances. Microbial infections, such as bacteria, viruses, and fungus, are the most common cause of pneumonia. On radiological imaging, distinguishing pneumonia caused by viruses, particularly COVID - 19, is a tough process that demands a great deal of knowledge and expertise in the field of radiology. The creation of computer vision-based tools for detecting COVID-19-associated radiological characteristics on radiological pictures of the lungs would be a very important tool to aid health professionals in their fight against this devastating infection that has afflicted the whole world. Radiologists will face a considerable challenge in identifying and correctly interpreting such minute changes because X-ray visual cues may be subtle. Therefore, having computer-aided diagnostic tools that can help radiologists evaluate X-ray changes that are indicative of COVID-19 more accurately and quickly becomes highly desirable and necessary. This project has two objectives. The CNN transfer learning approach was chosen because there weren't many images available for analysis. Researchers have proposed a simple CNN architecture with a modest number of parameters that successfully differentiates COVID-19 from conventional X-rays.

Related works

The segmentation of anomalies in COVID-19 chest CT images is proposed using Anam-Net, a lightweight CNN based on anamorphic depth embedding. The suggested Anam-Net is lightweight and ideal for inference generation in mobile or resource-constrained (point-of-care) systems because it has 7.8 times fewer parameters than the most recent UNet (or its variants) [1].

A different study suggests that the answers to these problems are a modified ResNet architecture for CT image classification as well as a revised MobileNet architecture for COVID-19 CXR image classification. Additionally, using CT scans and the suggested updated ResNet, the COVID-19, non-COVID-19 infections, and healthy controls are classified [2].

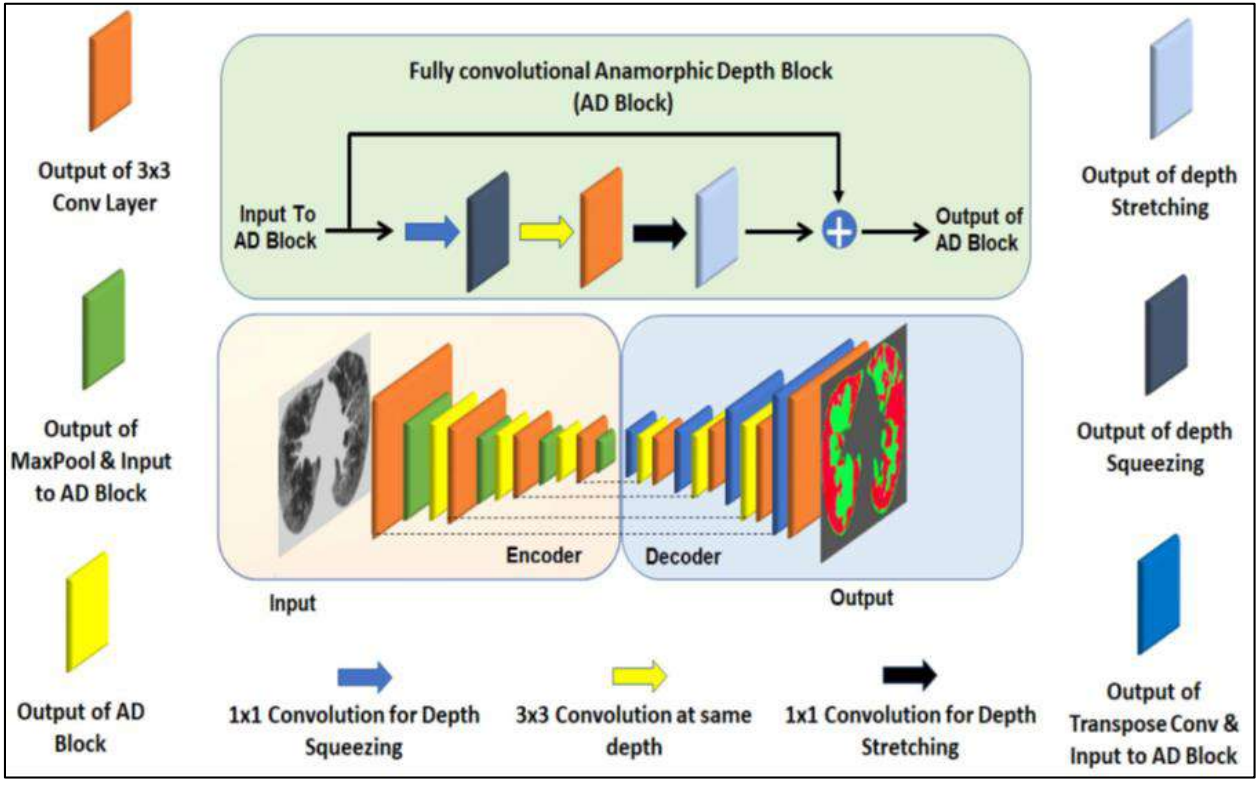

Fig 1: Anam-Net is a network design that is used to segregate anomalies in COVID-19 chest CT images [1].

In this study, a customised CNN architecture has been introduced to allow automated learning of such hidden properties. For each type of pneumonia, specific convolutional filter patterns are learned. To achieve this, a convolutional layer's many filters are constrained to only react maximally to a specific type of pneumonia/COVID-19. Enhancing the environment for discovering strong features and enhancing gradient movement between layers, the CNN design mixes different convolution types. The suggested work also visualises the X-ray zones of saliency that most significantly influenced CNN's prediction result [3].

i) They created and trained four CNN-RNN architectures to distinguish coronavirus infection from other infections.

ii) The dataset utilised to identify coronavirus patients consists of 6396 X-ray samples in total from diverse sources.

iii) The region under the receiver-operating characteristic characteristics (ROC) curve (AUC), accuracy, precision, F1-score, recall confusion matrix and Grad-CAM metrics are used to evaluate the performance of each design [6].

This study advances prior work in that it provides ANN-based lung segmentation, presents a hybrid structure made up of a BiLSTM layer with transfer learning, and achieves high classification performance. The contributions of the research are listed below.

- Automatic lung segmentation based on ANNs is employed to obtain robust features for the CNN-based transfer learning-BiLSTM network that will be used for the early diagnosis of COVID-19 infection, and
- To compare the suggested hybrid approach with other cutting-edge designs.
- The suggested model is simple, and it can detect COVID-19 totally on its own [8].

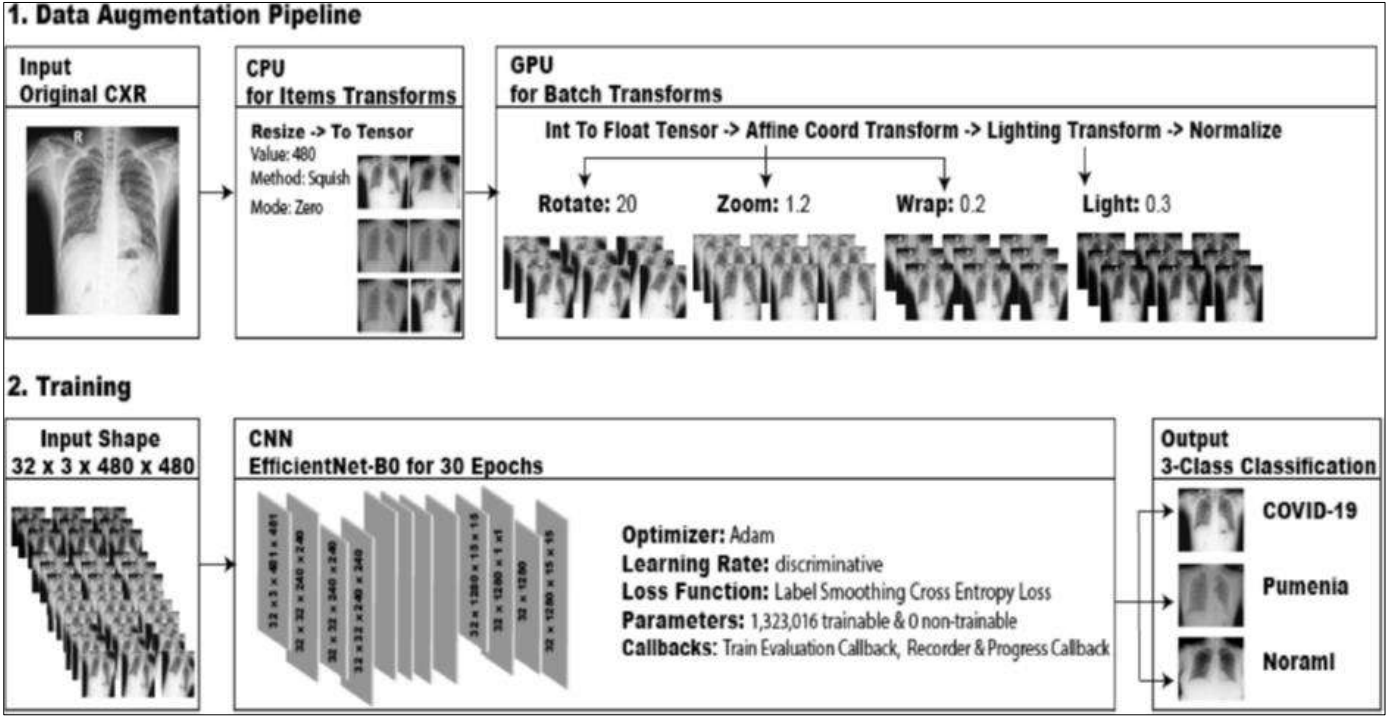

Fig 2: Covid Xray Net [9]

In this study, To identify the virus using chest X-rays, researchers create a hybrid deep learning algorithm based on a convolutional neural network (CNN) as well as a gated recurrent unit (GRU) (CXRs). A GRU serves as a classifier, while a CNN is used to extract features from the proposed model. Using 424 CXR images separated into three groups, the model was trained (COVID-19, Pneumonia, and Normal) [9]. In this paper, the validation accuracy of the CNN hyperparameters and data augmentation for COVID-19 identification from CXRs is improved. This innovation increases the accuracy of standard CNN architectures by 11.93% and 4.97%, respectively, for the Visual Geometry Group network (VGG-19) and the Residual Neural Network (ResNet-50). Following this, the CovidXrayNet model was proposed, that is based on the outcomes of our optimization and EfficientNet-B0. Two datasets were used to evaluate CovidXrayNet: the benchmark COVIDx dataset and the COVIDcxr dataset, which we produced (15,496 CXRs) [10].

Material and Method

A. Lung Extraction: Removing the lung area from chest CT scans is the first step in segmenting abnormalities. The lung masks from data were retrieved and displayed for convenient use. Using 231 training examples from a database of 5300 samples, a pretrained U-Net architecture that was trained with batch normalization to construct these lung masks was used.

B. Segmenting Medical Images Using Deep Learning: A shallow decoder was used to up sample the result while a deep encoder was employed to work on lower-resolution images and enable filtering techniques. Similar to this, another small-footprint solution known as LEDNet builds a module for asymmetric encoder-decoder on top of ResNet and includes a channel-wise split as well as shuffle operation for rapid and precise segmentation.

C. COVID-19 Anomaly Segmentation Techniques Proposed: The AD-final block's output, denoted by h(x), is produced by merging the feature mappings from the AD-input block's output of the series of convolution operations, denoted by f(x), parameterized by h, together with feature extraction, depth stretching, and depth squeezing. In a nutshell, $h(x)=f(x;h)+x$ [1].

For COVID-19 identification, they used VGG16, Inceptionv3, ResNet18 v1, DenseNet121, MobileNetv3 small, and SqueezeNet1.0. The matching kernels have a total of 7264 parameters. In the original MobileNet, the gradients' absolute values had a mean and a variance of 0.037 and 0.002,

respectively. The absolute value of the mean and variance values of gradients for the upgraded MobileNet are 0.547 and 0.551, respectively [2].

The dual residual connections across RCSDB block and CSDB block act as linked modules, resulting in various information flow net-work pathways. That is, the input features can follow any of the following paths: csdb conv1->rcsdb conv1, csdb conv1->rscdb conv2, csdb conv1->rscdb conv2, csdb conv2->rcsdb conv2. The modules gather and distribute contextual feature information over numerous channels and provide regularization capabilities in all of these available pathways (with dropout layers)

The suggested CNN is assessed on k-fold cross-validation (k=5folds) to establish model convergence on a small test dataset [3].

The two key stages of the suggested architecture for COVID-19 identification from CT-scan images are: constructing confidence ratings with several models, fusing the decision scores using the Gompertz function, and creating final predictions using a fuzzy rank-based technique [4].

Two CNN architectures are proposed for this project:

1) CNN with CSDB (channel-shuffled dual-branched)
2) CSDB CNN is a supplement to the Distinctive Filter Learning (DFL) paradigm. The CSDB CNN was created in order to suggest a network design that takes advantage of (1) dual residual connection across blocks, (2) connected network routes, (3) channel-shuffling, and (4) correlation of various receptive fields.

Using a single convolutional layer, The DFL module merely trains a number of class-identifying filters via a network learning technique. DFL seeks to quantify a metric of the filters' response to a target pneumonia class in order to minimise network loss [3].

This suggested method made use of balanced dataset with images of adult and young patients to learn the actual characteristics of the disease. To identify COVID-19 infection, the proposed approach includes many phases. In the pre-processing pipeline, chest X-ray samples were first scaled, shuffled, then normalised to identify the real features and minimize picture noise. Following that, A training set and a testing set were created from the dataset. We employed four pre-trained CNN architectures and an RNN classifier on the training dataset. The accuracy and loss of training datasets were calculated after each epoch, while the accuracy and loss of validation datasets were calculated using a five-fold cross-validation method [6].

A chest X-lung ray's area is assessed for COVID-19 detection. As a result, a detection that just includes the lung region in the image is more precise. In the raw photos, the locations of the lungs are not fixed. To segment the lung section, each image should be analysed separately. However, there are 2905 images in the COVID-19 radiography database. As a result, segmentation should be done automatically rather than manually. In this study, the classification process was limited to the lung region using ANN-based artificial segmentation.

50 pictures are fed into an autonomous segmentation software that uses the COVID-19, Normal, and Viral Pneumonia markers. Each selected image has three manual selection zones (bottom left, bottom right, and centre top). These three selection spots are then used to form the mask. Finally, the final image is created by multiplying the mask image with the original image. The final photos are then turned to grayscale [8].

Three blocks—the Conv-block, GRU-block, as well as FC-block—make up our network. We have a total of 5 Conv blocks, 1 GRU block, and 1 FC block. Two convolutional layers make up each Conv-block, and the last layer is a max-pooling layer. Following that, the GRU-Block receives the last conv-output block and extracts time information. The data is then passed to the final FC-block, which uses convolutional layers and a SoftMax function to forecast the illness [9].

To counteract the improper rotation of some of the obtained pictures, With a limit of 20 percent and a chance of 75 percent, we utilized a randomized rotation. We applied a scale of 1.2 zoom, a scale of 0.3 illumination, and a magnitude of 0.2 distortion with a probability of 75% to the CXRs. Patients seeing the X-ray instrument at different angles and in different lighting environments may benefit from warping and tightening augmentation. Efficient Net-head B0's was replaced with a head that was acceptable for three-class classification, and it was trained for 30 epochs [10].

Results

The average Dice score for the standard lung area was 0. 951, whereas the aberrant region had a score of 0. 68. In most cases, we found that the Dice score for the aberrant area was small (0.5) while processing the initial lung slices [1].

It should be noted that the recommended method exceeds the original MobileNet by achieving 99.7% test accuracy for classification into three categories, 99.9% for classification into four categories, and 99.6% for classification into three categories [2].

The proposed CSDB CNN classified the four target classes with an average accuracy of 93.42 percent. The model's precision, recall, F1-score, and accuracy values for the COVID-19 class were 95.93%, 92.50%, 94.10%, and 99.57%, respectively [3].

We used two publicly available datasets to assess the efficacy of the proposed method: the SARS-COV-2 dataset by Soares et al. 15 and the Harvard Data verse chest CT dataset35. The two data sets' distributions of images are not random [4].

The highest validation and training accuracy for the VGG19-RNN architecture is observed at 99.01% and 97.74%, while the loss is 0.02 and 0.09 at epoch 100. On the other side, the InceptionV3-RNN network has the lowest loss and training and validation accuracy (98.03 and 94.91 percent, respectively) (0.05 and 0.26 at epoch 100). When looking at the loss curve, compared to other networks, the loss values of the VGG19-RNN decrease more quickly and go closer to zero.

For COVID-19 cases, the VGG19-RNN network produced the best results, reaching 99.86% accuracy, 99.99% AUC, 99.78% precision, 99.78% recall, and 99.78% F1-score. Architecture InceptionV3-RNN, on the other hand, achieved a comparatively low performance with 98.56 percent accuracy, 99.95 percent AUC, 99.35 percent precision, 96.44 percent recall, and 97.87 percent F1-score. In addition, for all networks, ROC curves were built between the TP and FP rate. With AUCs ranging from 99.95 percent to 99.99 percent, the networks are able to differentiate COVID-19 patients from similar cases [6].

In the conclusion, the training and test losses both converge to the minimum of the graph. The training times for the CNN and BiLSTM networks are 2 minutes 19 seconds and 1 minute 25 seconds, respectively. But the above intervals are proportional to the number of iterations and epochs. For mAlexNet, the training process involves 1520 iterations, 5 epochs, and 139 seconds of training time. The hybrid architecture training consists of 1150 iterations and 50 epochs, and it lasts 224 (139 + 85) seconds. The suggested method is easy and quick to implement because of its end-to-end learning architecture because segmentation is carried out automatically without the need for a feature extraction step [8].

The 200th epoch, the acquired training as well as validation accuracy is 96.2 percent and 93.6 percent, respectively. Similarly, on the 200th epoch, training as well as validation loss are 0.8 and 0.9, respectively. Only three of the 28 photos in the pneumonia class were incorrectly identified as normal, while the remaining 25 photographs were correctly classified as pneumonia.

for each case in the test set, the precision, recall, and f1-score For typical class, GRU-CNN obtained 0.9 accuracy, 1.00 recall, and 0.95 f1-score. The accuracy, recall, and f1-score for COVID-19 are 1.00, 1.00, and 1.00, respectively. The accuracy, recall, and fi-score for pneumonia are 1.0, 0.89, and 0.94 [9],

Four COVID-19 patients were categorized as pneumonia by CovidXrayNet. The diagnosis is true, but the interpretation is wrong, because COVID-19 is a subgroup of pneumonia illnesses [10].

Discussion

The null result was successfully generated by the Anam-Net. In summary, Anam-Net requires less training time (approximately 43 percent less) than Attention UNet, and Anam-Net produces more accurate results than others [1].

The redesigned structure appears to address the over-fitting problem that plagued the original MobileNet for a variety of reasons [2].

The suggested approach has been convincingly tested on 112 samples using 5-fold cross-validation, resulting in higher 4-class accuracy [3].

Gompertz function-based fuzzy rank fusion using more in-depth data from various CNN modalities, combining many CNN base models. The frequency at which a negative quantity is confused for a positive one is known as the "False Positive Rate." Especially in the case of COVID-19 identification, the high prevalence of false-positives in medical data analysis can be problematic because misclassifying an infected patient as a non-infected case could lead to the predicted non-infected individual becoming a super-spreader, which could spread the disease more widely [4].

The diagnosis of COVID-19 infection was performed using four CNNs and an RNN. The findings showed that VGG19-RNN is more effective than other deep learning architectures at differentiating COVID-19 cases from normal cases and pneumonia cases. As a result, it is currently considered as a key deep learning architecture. The VGG19-RNN network outperformed pretrained CNN networks in terms of performance. According to studies, coronavirus infection can be distinguished using current technologies with an accuracy range of 80.6 to 98.3 percent. Contrarily, the accuracy of the VGG19-RNN network was 99.9%, which is higher than most contemporary systems. Last but not least, it is clear that the VGG19-RNN network outperformed other studies [6].

With more layers and parameters, SqueezeNet can attain the same degree of accuracy as other, more complex CNN architectures. On the ImageNet dataset, for example, SqueezeNet may match Alex-accuracy Net's performance

while utilising 50X less parameters as well as a model size little less than 0.5MB. "Fire Module" blocks make up the SqueezeNet. In an expanding section, two convolution layers by using 1x1 and 3x3 filters in each block are fed by a squeeze convolution layer (with 1x1 filters). A ReLU layer [7].

Individual data augmentation techniques only marginally improved task performance. For instance, the ideal warping setting increases classification task accuracy by just 1.56%. However, performance was significantly enhanced by combining these better methods (such as our suggested data augmentation pipeline and CNN hyperparameters). It increases the accuracy of well-known CNN designs by 11.93% and 4.97%, respectively, for VGG-19 and ResNet-50 [10].

Conclusion

The results of the three studies' test subjects' chest CT images revealed that the suggested strategy was capable of obtaining high Dice similarity scores for both sick and healthy areas. The Anam-Net was also contrasted with a number of cutting-edge lightweight and heavy networks, including ENet, UNet++, SegNet, Attention UNet, LEDNet [1].

Two new models and six commonly used deep learning algorithms made specifically for COVID-19 recognition are contrasted with the suggested method. According to the results of our comparison research, the updated CNN design appears to function well, indicating that it might be used for computer-aided diagnosis of COVID-19 positive patients in clinical settings [2].

The present feature map's first-order gradients are softmax weighted in the unique convolutional filter learning module's recommendation to create notable features. Different sets of filters are adjusted to learn unique patterns for each pneumonia class using weighted gradients as a metric of filter affinity towards the predicted class [3].

Additionally, a fully automated COVID-19 detection system built on deep learning was described. This framework classifies chest CT-scan images rather than time-consuming RT PCR tests, which is a more accessible option.

This demonstrated how to use decision scores produced from various CNN models to locate COVID-19 cases using fuzzy rank-based fusion. The suggested technique is the first of its kind to use the Gompertz function to build an ensemble model for COVID-19 identification. On the SARS-COV-2 as well as Harvard Dataverse datasets, the suggested technique worked remarkably well, with low false-positive rates, higher recognition accuracies of 98.93 and 98.80 percent, and sensitivities of 98.930 and 98.80 percent [4].

A new CNN architecture as well as a network learning methodology were reported for classifying COVID-19 from chest X-rays. CNN learns strong features using channel shuffle and dual residual skip connections. Dual branching is combined with many convolutional layers to raise a variety of contextual features. The CNN architecture effectively combines receptive fields of different sizes and upholds a constant gradient flow between blocks. The proposed unique convolutional filter learning module employs softmax weighting on the first-order gradients of the active feature map to produce noteworthy features [3].

Using CNN, deep transfer learning, and RNN, it classified the COVID-19, pneumonia, and normal categories for the X-ray samples. Based on the attributes that were taken from the four most well-known CNN networks, the RNN network was used to categorise different classes. With 99.91% accuracy, 99.92% AUC, 99.82% recall, and 99.85% F1- score, the VGG19- RNN is recognised as the finest network for identifying COVID-19 cases. The doctor's workload should ideally be lessened while examining COVID-19 occurrences [6].

It offers a CNN architecture for distinguishing COVID-19 from other CT images that is based on the SqueezeNet CNN model (composed both by community-acquired pneumonia and healthy images). The suggested CNN-2 outperforms the original SqueezeNet on both dataset setups. CNN-2 had an accuracy of 85.03 percent, a sensitivity of 87.55 percent, a specificity of 81.95 percent, a precision of 85.01 percent, and an F1-Score of 86.20 percent. Additionally, CNN-2 outperforms older, more complex CNN models in terms of performance. In reality, a medium-end laptop and a high-end computer both have quick average classification times (1.25 seconds for a single CT scan). This shows that even with constrained hardware resources, the highly recommended CNN can analyse hundreds of photos every day [7].

GRU served as the classifier, and CNN served as the feature extractor. Combining retrieved characteristics with GRU enhances the efficacy of the proposed method for classification between COVID, pneumonia, and normal occurrences [9].

Revealed that maximizing data augmentation and CNN hyperparameters has a significant impact on the automated extrac-tion of COVID-19-related features from CXR. On the COVIDx dataset, Cov-idXrayNet needs just 30 learning cycles to analyze a CXR and achieves 95.82 percent accuracy [10].

References

1. Anam-Net: Anamorphic Depth Embedding-Based Light weight CNN for Segmentation of Anomaliesin COVID-19 Chest CT Images Naveen Paluru, Aveen Dayal, Håvard Bjørke Jenssen, Tomas Sakinis, Linga Reddy Cenkeramaddi, Senior Member, IEEE, Jaya Prakash, and Phaneendra K. Yalavarthy, Senior Member, IEEE
2. Classification of COVID-19 chest X-Ray and CT images using a type of Dynamic CNN modification Method Guangyu Jia, Hak-Keung Lam*, Yujia Xu
3. Fuzzy rank-based fusion of CNN models using Gompertz function for screening COVID-19 CT-scans. Rohit Kundu, Hritam Basak, Pawan Kumar Singh, AliAhmadian, Massimiliano Ferrara & Ram Sarkar.
4. Learning distinctive filters for COVID-19 detection from chest X-ray using shuffled residual CNN. R. Karthik, R. Menaka, Hariharan M.
5. Diagnosis of COVID-19 from X-rays Using Combined CNN-RNN Architecture with Transfer Learning. Mabrook S. Al-Rakhami, Md. Milon Islam, Md. Zabirul Islam, Amanullah Asraf, Ali Hassan Sodhro, Weiping Ding.
6. A Light CNN for detecting COVID-19 from CT scans of the chest. Matteo Polsinelli, Luigi Cinque, Giuseppe Placidi
7. CNN-based transfer learning– BiLSTM network: A novel approach for COVID-19 infection detection. Muhammet Fatih Aslan, Muhammed Fahri Unlersen, Kadir Sabanci, Akif Durdu.
8. Deep GRU-CNN model for COVID-19 detection from chest X-rays data Pir Masoom Shah, Faizan Ullah, Dilawar Shah, Abdullah Gani (Senior Member, IEEE), Carsten Maple (Member, IEEE), Yulin Wang, Shahid, Mohammad Abrar, Saif Ul Islam
9. Covid Xray Net: Optimizing data augmentation and CNN hyperparameters for improved COVID-19 Detection from CXR Maram Mahmoud A. Monshia, Josiah Poon A, Vera Chung A, Fahad Mahmoud Monshi